# A bi-monomeric, nonlinear Becker-Döring-type system to capture oscillatory aggregation kinetics in prion dynamics

Marie Doumic* Klemens Fellner† Mathieu Mezache‡ Human Rezaei§

August 29, 2018

**Abstract**

In this article, in order to understand the appearance of oscillations observed in protein aggregation experiments, we propose, motivate and analyse mathematically the differential system describing the kinetics of the following reactions:

$$\begin{cases} \mathcal{V}+\mathcal{W} & \xrightarrow{k} & 2\mathcal{W}, & \\ \mathcal{W}+\mathcal{C}_i & \xrightarrow{a_i} & \mathcal{C}_{i+1}, & 1\le i\le n, \\ \mathcal{C}_i+\mathcal{V} & \xrightarrow{b_i} & \mathcal{C}_{i-1}+2\mathcal{V}, & 2\le i\le n, \end{cases}$$

with $n$ finite or infinite. This system may be viewed as a variant of the seminal Becker-Döring system, and is capable of displaying sustained though damped oscillations.

**Keywords:** Protein polymerisation, Prion modelling, Becker-Döring system, Lotka-Volterra system, Lyapunov functional, stability analysis, oscillations, asymptotic expansion.

**Mathematical Subject Classification:** 34E05, 34D08, 37L15, 92B05

## 1 Introduction

The aim of this article is to propose and study a new polymerisation-depolymerisation model capable of explaining oscillations, which have been observed experimentally in the time-course of

*Sorbonne Universités, Inria, Université Paris-Diderot, CNRS, Laboratoire Jacques-Louis Lions, F-75005 Paris, France, marie.doumic@inria.fr - Wolfgang Pauli Institute, c/o university of Vienna, Austria

†University of Graz, Austria, Institute of Mathematics and Scientific Computing, 8010 Graz, klemens.fellner@uni-graz.at

‡Sorbonne Universités, Inria, Université Paris-Diderot, CNRS, Laboratoire Jacques-Louis Lions, F-75005 Paris, France,mathieu.mezache@inria.fr

§INRA, UR892, Virologie Immunologie Moléculaires, 78350 Jouy-en-Josas, France, human.rezaei@inra.fr

prion protein polymerisation experiments. Up to our knowledge, such oscillations have never been observed, neither theoretically or numerically, in the family of growth-fragmentation-nucleation equations, which are most often used to model protein polymerisation.

## Biological background and motivation

In its largest acceptance, the prion phenomenon (prion being derived from 'proteinaceous infectious only particle') involves the self-propagation of a biological information through structural information transfer from a protein in a prion-state (i.e. misfolded resp. infectious) to the same protein in a non-prion state. Such a concept is key to the regulation of diverse physiological systems and to the pathogenesis of prion diseases [9, 24, 26]. Recently, prion-like mechanisms have been involved in the propagation and gain of toxic functions of proteins or peptides associated with other neurodegenerative disorders such as Alzheimer, Parkinson and Huntington diseases [17]. Elucidating the mechanisms driving prion-like aggregation is thus of key importance, and, as explained below, still requires new mathematical modelling and analysis.

During the evolution of prion pathology, the host encoded monomeric prion protein (PrPC) is converted into misfolded aggregating conformers (PrPSc) [6]. PrPSc assemblies have the ability to self-replicate and self-organise in the brain through a still unresolved molecular mechanism commonly called *templating*. Differences in disease phenotypes (distinctive symptomologies, incubation times, and infectious characters of PrPSc) are reported within the same host species. These phenotypic differences are assigned to structural differences in PrPSc assemblies, introducing the concept of *prion strains* based on structural diversity/heterogeneity of PrPSc assemblies. In the prion literature a plethora of evidences strongly suggest that within a given prion strain a PrPSc structural heterogeneity exists, which suggests that in a given environment structurally different PrPSc subassemblies with different biological and physico-chemical properties coexist [18] even if the mechanism of this diversification remains elusive. To date, very few mathematical models have taken into account the coexistence of multiple prion assemblies or multiple type of fibrils [10]. Indeed, most of the aggregation models have been built using the canonical nucleation-elongation-fragmentation process seminally reported by Bishop and Ferrone (see e.g. [5, 19, 23]), which is based on the existence of a structurally unique type of assemblies characterised only by their size distribution. The characterisation of multiple types of PrPSc subassemblies with different rates of aggregation, depolymerisation and exchange requires new mathematical models and analyses to describe the dynamics and relation between different subspecies.

In order to explore the consequence of the coexistence of structurally different PrPSc assemblies within the same environment, the depolymerisation kinetics of recombinant PrP amyloid fibrils have been explored by Static Light Scattering (SLS) [20]. A detailed study of those experiments revealed a surprising, transient oscillatory phenomenon as the time evolution of the SLS measurement (see Appendix D for details) shows in Figure 1: First note that when denoting by $c_i(t)$ the concentrations at time $t$ of the polymers containing $i$ monomers, we can interpret

the signal of an experimental SLS measurement, as in [23], as the time evolution of the second moment of the polymers, *i.e.*

$$M_2(t) := \sum_{i=1}^{n} i^2 c_i(t). \tag{1}$$

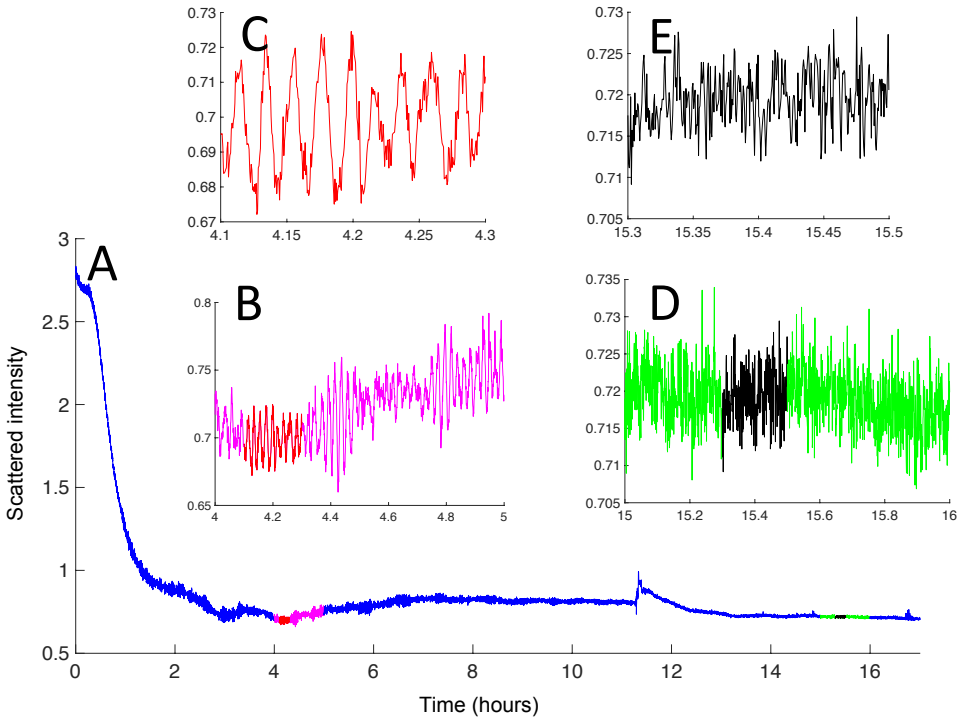


Figure 1: Human PrP amyloid fibrils (Hu fibrils) depolymerisation monitored by Static Light Scattering (see Appendix D for details). A: The overall view of the $0.35\mu M$ Hu-fibrils depolymerisation at $55^0C$. B-E correspond to a zoom-in on different time-segments of the depolymerisation curve A. As shown in B, from time 4 to time 5h oscillations have been observed when for time segment corresponding to time 15.3 to 15.5h only noise has been detected (D).

Hence, at the beginning of the experiments, after a short lag phase, quick depolymerisation is observed. This is followed by a transient phase ranging from approximately 1h to 11 hours, when slow variations were superimposed by fast periodic oscillations with a frequency around 0.01 to 0.02 Hz, see Figures 1B and 1C. Both the variations and the oscillations progressively

disappear, and a constant signal with noise is observed at the end of the experiments (Figure 1, D and E). This specific phenomenon may be used to gain new insight into the underlying biological mechanism.

A first key question of our study is thus the following: What kind of core elements should a model feature in order to explain the appearance of such oscillations?

The most natural departure point in the formulation of a suitable mathematical model is the Becker-Döring model of polymerisation and depolymerisation [4]. The Becker-Döring model is coherent with other biological measurements [20], and it is viewed in the protein polymerisation literature as the "primary pathway" model [5, 23].

Becker-Döring considers two reverse reactions: polymerisation through monomer addition, and depolymerisation due to monomer loss. Accordingly, the model is characterised by the following system of reactions, where $\mathcal{C}_i$ denotes polymers containing $i$ monomers - so that $\mathcal{C}_1$ are the monomers - and $a_i$, $b_i$ are the polymerisation resp. depolymerisation reaction rate coefficients:

$$\begin{cases} \mathcal{C}_1 + \mathcal{C}_i \xrightarrow{a_i} \mathcal{C}_{i+1}, & i \geq 1, \\ \mathcal{C}_i \xrightarrow{b_i} \mathcal{C}_{i-1} + \mathcal{C}_1, & i \geq 2. \end{cases}$$

The Becker-Döring system, however, satisfies the detailed balance condition [3], which implies the existence of a Lyapunov functional and no sustained oscillations are possible. Also damped oscillations, up to the best of our knowledge, have never been observed numerically or evidenced analytically. We thus needed a variant of the Becker-Döring model to explain the experimentally observed oscillations displayed in Figure 1.

In [16], it was recently shown that PrPSc assemblies are in equilibrium with an oligomeric conformer (suPrP) encoding the entire strain information and constituting an elementary building block of PrPSc assemblies. The fact that such an oligomeric building block appears separately from the monomeric PrP points towards models with two different quasi-monomeric species (i.e. one monomer and one oligomeric conformer in contrast to the polymer species $\mathcal{C}_i$), each of which playing a role in a different reaction. A suitable mathematical model should also to take into account the constraint that large polymers cannot interact directly, for reasons of size and order of magnitude of their concentrations. Hence, we assume that polymers can only interact indirectly, through the exchange of monomers or small oligomeric conformers.

A third crucial modelling aspect concerns the details of the depolymerisation reaction rates, which are linear in the original Becker-Döring system. However, numerical studies (see below for a more detailed discussion and numerical illustrations) as well as the content of this paper strongly suggests that sustained or damped oscillations require a nonlinear (more precisely, a monomer induced) depolymerisation process, which we detail in the following Section.

## 2 Introduction of the proposed model system

We propose the following model system: Let $\mathcal{V}$ and $\mathcal{W}$ denote the two monomeric species, where the second, conformer species is taken monomeric for the sake of simplicity (but a slight modification of the model would allow to consider it as oligomeric). Let $\mathcal{C}_i$ be the polymers containing $i$ monomers, where polymerisation signifies the amendment of a monomer $\mathcal{W}$ while depolymerisation only occurs when induced via the monomeric species $\mathcal{V}$. More precisely, we consider

$$\begin{cases} \mathcal{V}+\mathcal{W} & \xrightarrow{k} & 2\mathcal{W}, & \\ \mathcal{W}+\mathcal{C}_i & \xrightarrow{a_i} & \mathcal{C}_{i+1}, & 1\le i\le n, \\ \mathcal{C}_i+\mathcal{V} & \xrightarrow{b_i} & \mathcal{C}_{i-1}+2\mathcal{V}, & 2\le i\le n. \end{cases} \tag{2}$$

with a reaction rate constant $k$ for the monomer/conformer dynamics and polymerisation/depolymerisation coefficients $a_i$ and $b_i$. Note that large values for $k$ compared to $a_i$, $b_i$ introduce a slow-fast behaviour into (2) and yields a mechanism of oscillations which is detailed in a fully rigorous way for a two-polymer system (i.e. $n=2$) in Section 3.

We emphasise the two main differences of (2) compared to the classical Becker-Döring system: First, instead of one monomeric species $\mathcal{C}_1$, we now consider two interacting species of monomers (or conformers), $\mathcal{V}$ and $\mathcal{W}$. Secondly, depolymerisation is modelled as a monomer induced, nonlinear process, which requires the catalytic action of $\mathcal{V}$. Note that this process is reminiscent of the cyclical behaviour of the three-species system

$$\mathcal{V}+\mathcal{W} \xrightarrow{k} 2\mathcal{W}, \qquad \mathcal{W}+\mathcal{M} \xrightarrow{a} 2\mathcal{M}, \qquad \mathcal{M}+\mathcal{V} \xrightarrow{b} 2\mathcal{V}, \tag{3}$$

which is known to produce sustained periodic oscillations, see [28], where it is called the Ivanova system, or [27], where it is referred to as a simplification of the Belousov-Zhabotinsky system.

To reiterate and further illustrate the reasons which guided us towards model (2), let us isolate those two main ingredients. Firstly, let us modify the Becker-Döring system by taking two monomeric species [16], but with a standard linear depolymerisation reaction, i.e. we consider the following system:

$$\begin{cases} \mathcal{V}+\mathcal{W} & \xrightarrow{k} & 2\mathcal{W}, & \\ \mathcal{W}+\mathcal{C}_i & \xrightarrow{a_i} & \mathcal{C}_{i+1}, & 1\le i\le n, \\ \mathcal{C}_i & \xrightarrow{b_i} & \mathcal{C}_{i-1}+\mathcal{V}, & 2\le i\le n. \end{cases} \tag{4}$$

Figure 2 compares the behaviours of the bi-monomeric Becker-Döring system (4) to model (2) under conditions when both feature oscillations (which is systematic in the nonlinear depolymerisation model (2), yet only occurs for some parameters in the bi-monomeric Becker-Döring system (4)). Nevertheless, even if the bi-monomeric Becker-Döring system (4) shows oscillatory behaviour, those oscillations are far less sustained and cannot serve as an explanation of the experimental observations.

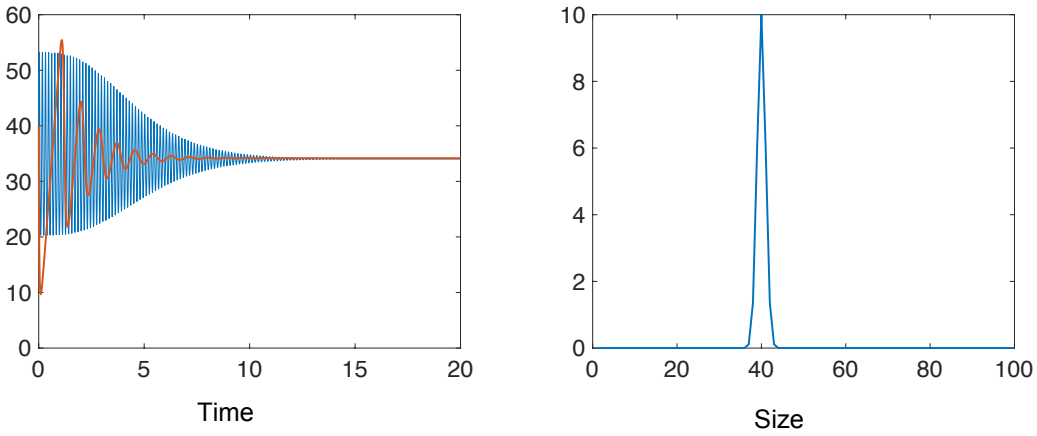


Figure 2: Left images: Comparison of the oscillatory behaviour of the monomer concentration $v$ of the proposed model (2) (blue) with the bi-monomeric Becker-Döring system (4) with linear depolymerisation (red) subject to the same initial distribution (Right image).

Interestingly, nonlinear depolymerisation leads not only to much more sustained oscillations, but also yields faster convergence to its size-distribution equilibrium (data not shown), while the linear bi-monomeric Becker-Döring system (4) exhibits similar metastability as observed for the Becker-Döring system [21].

Secondly, when considering a monomeric Becker-Döring system with second-order depolymerisation reaction:

$$\mathcal{V}+\mathcal{C}_i \quad \xrightarrow{a_i} \quad \mathcal{C}_{i+1}, \quad 1\le i\le n, \qquad \mathcal{C}_i+\mathcal{V} \quad \xrightarrow{b_i} \quad \mathcal{C}_{i-1}+2\mathcal{V}, \quad 2\le i\le n, \tag{5}$$

numerical simulations do not display any kind of oscillations, see second row in Figure 3.

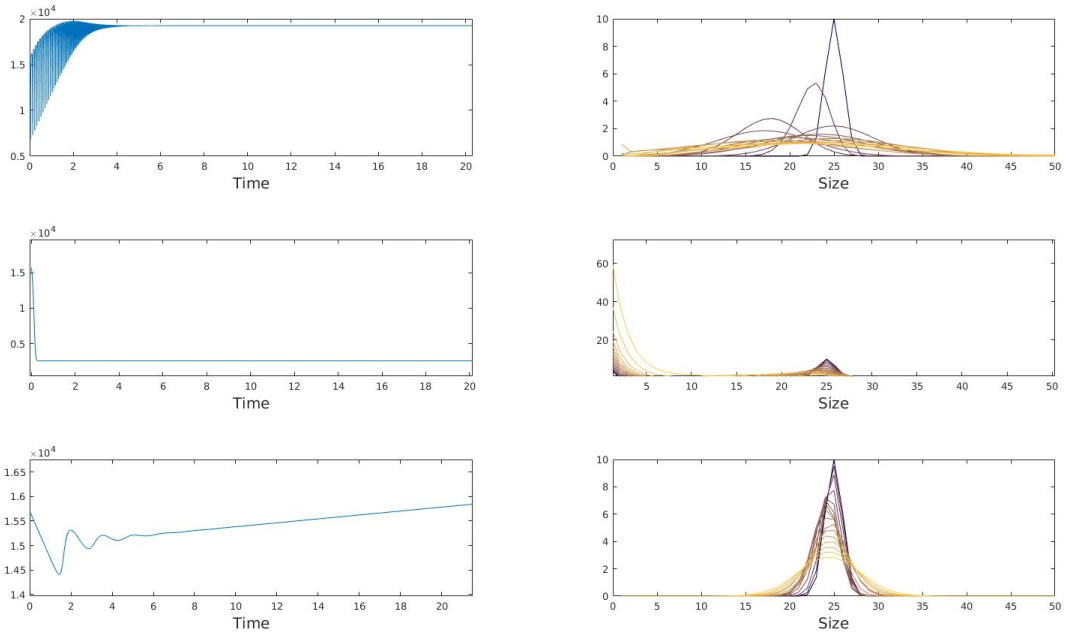


Figure 3: Numerical results corresponding to SLS measurement, *i.e.* the quantity $M_2$ defined by (1) (Left Column) and the evolution of the size distribution of polymers (Right Column). First Row: The here proposed model (2) with parameters $n = 50$, $k = 9.5$, $a_i = 4.8$, $b_i = 8$. Second Row: The model (5) with $c_1$ multiplied by 10 in order to ignite the reactions in the system. Third row: The model (4) with parameters $n = 50$, $k = 0.95$, $a_i = 0.48$, $b_i = 0.8$.

Let us also remark that in model (2), the first polymer species $\mathcal{C}_1$ could also denote a smallest polymer of size $n_0 > 1$, i.e. it represents the smallest "active" polymer size. This means that no nucleation, as modelled by $\mathcal{C}_1 + \mathcal{C}_1 \to \mathcal{C}_2$ in the Becker-Döring system, is considered. This is in

line with the time-scale of the considered experiment where nucleation is negligible compared with other reactions.

Finally, the original Becker-Döring system (for $n = \infty$) allows to model phase transitions where polymers of infinite size are created in finite time depending on the polymerisation coefficients; a phenomenon called *gelation* or also *Ostwald ripening* [3]. In this paper, we shall consider both finite or infinite systems and discuss similarities and differences. However, in view of our application background of understanding amyloid fibrils, we are never interested in the appearance of gelation or Ostwald ripening and only consider polymerisation coefficients, where the average size of polymers, though possibly large, remains finite.

The purpose of this article is to provide a first insight into this new, in our opinion highly promising model. In particular, model system (6) in the following section reveals extremely rich behaviour and is capable of displaying various types of dynamics such as sustained and damped periodic oscillations.

### 2.1 A bi-monomeric nonlinear Becker-Döring model: Formal properties

We denote by $c_i(t)$, $v(t)$ and $w(t)$ the concentrations at time $t$ of the polymers containing $i$ monomers, the depolymerising and the polymerising monomeric species. We assume the reactant's concentrations to be sufficiently large to neglect stochastic effects and consider a deterministic setting. By using the mass-action law, model (2) yields the following system of differential equations:

$$\begin{cases} \frac{dv}{dt} = -kvw + v\sum_{i=2}^{n} b_i c_i, & v(0) = v^0, \\ \frac{dw}{dt} = -w\sum_{i=1}^{n-1} a_i c_i + kvw, & w(0) = w^0, \\ \frac{dc_1}{dt} = -wa_1c_1 + vb_2c_2, & c_1(0) = c_1^0, \\ \frac{dc_i}{dt} = w(-a_ic_i + a_{i-1}c_{i-1}) + v(b_{i+1}c_{i+1} - b_ic_i), \quad 2 \le i \le n-1, & c_i(0) = c_i^0, \\ \frac{dc_n}{dt} = wa_{n-1}c_{n-1} - vb_nc_n, & c_n(0) = c_n^0, \end{cases}$$

where the last equation is only to be considered when $n$ is finite.

As in [22], we introduce the net rate of an $i$-polymer being converted to an $(i+1)$-polymer by

$$J_i = wa_ic_i - vb_{i+1}c_{i+1}, \qquad 1 \le i \le n-1.$$

With the convention $J_0 = J_n = 0$, we can thus rewrite the above system as

$$\begin{cases} \frac{dv}{dt} &= -kvw + v\sum_{i=2}^{n} b_i c_i, & v(0) = v^0, \\ \frac{dw}{dt} &= -w\sum_{i=1}^{n-1} a_i c_i + kvw, & w(0) = w^0, \\ \frac{dc_i}{dt} &= J_{i-1} - J_i, & c_i(0) = c_i^0, \quad 1 \le i \le n. \end{cases} \tag{6}$$

In this paper, we shall always assume the initial conditions and reaction rates to be such that there exists a unique solution $(v, w, c_i) \in \mathcal{C}^1(0,T)^2 \times \mathcal{C}^1(0,T,\ell^1_1)$, where we denote

$$\ell^1_s := \left\{ (x_i)_{i\ge 1} \in \mathbb{R}^{\mathbb{N}} \;\middle|\; \sum_{i\ge 1} i^s x_i < \infty \right\}, \qquad \text{for} \quad s \in \mathbb{R}\,.$$

We first remark that solutions to system (6) in $\ell^1_1$ have two conserved quantities, obtained by weighted sums of the equations:

1. The total number of polymers, since $\frac{d}{dt}\sum_{i=1}^n c_i = 0$. This conservation law is linked to the fact that we neglect nucleation.
2. The total mass, since $\frac{d}{dt}\big(v + w + \sum_{i=1}^n i c_i\big) = 0$, which indicates that there is no gain or loss of particles during the chemical reactions: the system is closed.

As a consequence of those two conservation laws, we introduce

$$P_0 := \sum_{i=1}^{n} c_i^0, \qquad M_{tot} := v^0 + w^0 + \sum_{i=1}^{n} i c_i^0.$$

**Overview:** The manuscript is organised from the simplest to the most complete cases: In Section 3, we provide a complete and explicit study of the two-polymer case $n = 2$, which features a pivotal mechanism of damped periodic oscillations in the case of a large reaction rate $k$ compared to the polymerisation coefficients, see Corollary 1. To understand this mechanism, Theorem 1 states the existence of a Lyapunov functional, which is also the Hamiltonian of an underlying Lotka-Volterra models and proves exponential convergence to an equilibrium of solutions despite their highly oscillatory behaviour, see e.g. the left blue solution in Figure 2. The main difficulty lies in the fact that the time derivative of the Lyapunov functional vanishes across some lines in phase-space, which necessitates precise estimates.

In Section 4, we focus on the case where the maximal size of polymers $n$ is finite. We study the existence of steady states and their stability (Proposition 1). Further details are obtained in the case of constant coefficients, where we discuss the various zones of stability or instability with respect to the parameters.

In the final Section 5, we analyse well-posedness and steady states of the infinite system $n = \infty$. Two specific cases shed light on the damped oscillations: the constant coefficient case (i.e. $a_i = a,\ b_i = b$ for two positive constants $a$ and $b$ and for all $i$) and the linear coefficient case (where $a_i = ia$, $b_i = (i-1)b$, for two positive constants $a$ and $b$ and for all $i$).

# 3 The two-polymer model

In this section, we study the bi-monomeric system (2) coupled to only two sizes of polymers in the case of normalised coefficients $a_1 = b_2 = 1$ for the sake of the clearest possible presentation. We thus investigate the following two-polymer model

$$\begin{cases} \frac{dv}{dt} = v\left[-kw + c_2\right], \\ \frac{dw}{dt} = w\left[kv - c_1\right], \end{cases} \qquad \begin{cases} \frac{dc_1}{dt} = -wc_1 + vc_2, \\ \frac{dc_2}{dt} = wc_1 - vc_2, \end{cases} \tag{7}$$

subject to the nonnegative initial data $v(0) = v^0$, $w(0) = w^0$, $c_1(0) = c_1^0$ and $c_2(0) = c_2^0$.

The purpose of this section is to explicitly exemplify a mechanism of transient oscillatory behaviour of (2) under the assumption that the reaction rate constant $k$ is large (compared to the other parameters). More precisely, for a sufficiently small parameter $\varepsilon = \frac{1}{k}$, we will prove that under general conditions solutions to (7) converge exponentially to a positive equilibrium state while undergoing $O(1/\varepsilon)$ many transient oscillations.

This result is a consequence of proving that the two-polymer model (7) i) features a convex Lyapunov functional which entails exponential convergence to equilibrium via a generalised entropy method and ii) can be reformulated as a regular perturbation of a classical Hamiltonian-conserving Lotka-Volterra system, for which the perturbative terms are of order $\varepsilon$ and cause exponential convergence to equilibrium on a time scale of order $1/\varepsilon$.

First, we recall that system (7) conserves the total number of polymers and the total mass. This implies the following two mass conservation laws for all $t \geq 0$:

$$c_1(t) + c_2(t) = P_0 = c_1^0 + c_2^0, \qquad \text{and} \qquad v(t) + w(t) + c_2 = M_{tot} - P_0 =: M.$$

Expressing $c_1$ and $c_2$ in terms of these two conservation laws allows to reduce system (7) into

$$\begin{cases} \frac{dv}{dt} = v\left[M - (k+1)w - v\right], \\ \frac{dw}{dt} = w\left[(M - P_0) + (k-1)v - w\right], \end{cases} \tag{8}$$

which constitutes a generalised Lotka-Volterra system of predator-pray type, see e.g. see [7] or [15], for which possible behaviours have been extensively listed and studied, and for which convergence may either be proved using an appropriate Lyapunov functional or using the Poincaré-Bendixson theorem and the Poincaré-Dulac theorem. However, up to our knowledge, those methods do not provide a rate of convergence or explicit estimates.

Besides the boundary equilibria $(\bar{v}, \bar{w}) = (M, 0)$ and $(\bar{v}, \bar{w}) = (0, M - P_0)$ (in case $M \geq P_0$), system (8) satisfies the equilibrium

$$v_\infty := \frac{P_0}{k}\left(1 + \frac{1}{k}\right) - \frac{M}{k}, \qquad w_\infty := \frac{M}{k} - \frac{P_0}{k^2},$$

and $(v_\infty, w_\infty) > 0$ provided that $P_0 \in \left(\frac{kM}{1+k}, kM\right)$, which we shall assume henceforth.

We observe that the equilibrium $(v_\infty, w_\infty)$ takes values of order $\varepsilon := 1/k$. This suggests the rescaling

$$v \to \frac{v}{k} = \varepsilon v, \qquad \text{and} \qquad w \to \frac{w}{k} = \varepsilon w,$$

and yields the rescaled equilibrium values

$$v_\infty = P_0\,(1 + \varepsilon) - M, \qquad \text{and} \qquad w_\infty = M - \varepsilon P_0, \tag{9}$$

By using (9) and $v_\infty + w_\infty = P_0$, system (8) rescales to the following two-polymer system, which we shall study subsequently:

$$\begin{cases} \frac{dv}{dt} = v\,[w_\infty - w] - \varepsilon\, v\,[v - v_\infty + w - w_\infty]\,, \\ \frac{dw}{dt} = w\,[v - v_\infty] - \varepsilon\, w\,[v - v_\infty + w - w_\infty]\,. \end{cases} \tag{P2}$$

First, we point out that the rescaled two-polymer model (P2) in the limiting case $\varepsilon = 0$ constitutes a classical Lotka-Volterra system, i.e.

$$\begin{cases} \frac{dv_0}{dt} = v_0\,[w_\infty - w_0] = v_0\, w_0\big(-\frac{\partial H}{\partial w_0}\big), \\ \frac{dw_0}{dt} = w_0\,[v_0 - v_\infty] = w_0\, v_0 \frac{\partial H}{\partial v_0}, \end{cases} \tag{10}$$

which is defined by and conserves the Hamiltonian

$$\begin{aligned} &H(v, w) = v - v_\infty \ln v + w - w_\infty \ln w \\ &\frac{d}{dt} H(v_0(t), w_0(t)) = \frac{\partial H}{\partial v}\frac{dv_0}{dt} + \frac{\partial H}{\partial w}\frac{dw_0}{dt} = 0. \end{aligned} \tag{11}$$

Moreover, for positive equilibria $(v_\infty, w_\infty) > 0$, the Hamiltonian $H$ is the sum of the convex functions $v - v_\infty \ln v$ and $w - w_\infty \ln w$ with minima at $v_\infty$ and $w_\infty$. Hence, any positive equilibrium $(v_\infty, w_\infty) > 0$ is the unique minimiser of the associated Hamiltonian (11) and $H(v, w) > H(v_\infty, w_\infty)$ for all $(v, w) \neq (v_\infty, w_\infty)$.

### 3.1 Large-time behaviour and entropy functional

The following theorem proves large-time convergence to the positive equilibrium $(v_\infty, w_\infty)$ by using that the Hamiltonian (11) is a Lyapunov functional to the full system (P2).

**Theorem 1** (Exponential convergence to positive equilibrium)**.**
*Consider $P_0 \in \left(\frac{kM}{1+k}, kM\right)$ and hence a positive equilibrium $(v_\infty, w_\infty) > 0$.*

*Then, the Hamiltonian* (11) *is a convex Lyapunov functional for system* (P2) *with a decay rate of order $\varepsilon$. More precisely,*

$$\frac{d}{dt}H(v(t), w(t)) = -\varepsilon\, p^2(v(t), w(t)), \quad \text{with} \quad p(v, w) := \left[(v - v_\infty) + (w - w_\infty)\right]. \tag{12}$$

*Moreover, for $\varepsilon$ sufficiently small, every solution $(v(t), w(t))$ to* (P2) *subject to positive initial data $(v_0, w_0) > 0$ converges exponentially to the positive equilibrium $(v_\infty, w_\infty)$, i.e.*

$$|v - v_\infty|^2 + |w - w_\infty|^2 \le C\left(H^0 - H_\infty\right) e^{-\varepsilon r t}, \tag{13}$$

*where the positive rate $r$ and constant $C$ depend only on the initial value of the Hamiltonian $H^0 := H(v^0, w^0)$ and the values of the positive equilibrium $(v_\infty, w_\infty)$.*

**Proof.** The decay rate of the Hamiltonian (12) follows from direct calculations when evaluating $H$ along the flow of (P2).

In the following, we prove the exponential convergence (13) via a modified entropy method. The standard entropy method consists in proving a functional inequality, which bounds the entropy production functional (i.e. the entropy decay rate) below in terms of the relative entropy to equilibrium, see e.g. [**?**, 11, 12, 13] in the context of nonlinear reaction-diffusion system. For the present Hamiltonian decay (12), however, this approach would aim for an estimate like $p^2(v, w) \ge r(H(v, w) - H_\infty)$ for a rate $r > 0$, which cannot hold since $p^2$ vanishes at a straight line through the equilibrium point:

$$p = 0 \quad \Longleftrightarrow \quad w - w_\infty = -(v - v_\infty).$$

In order to still prove exponential convergence to equilibrium, we shall provide estimates, which show that all solution trajectories pass through this line of degeneracy with positive speed. We first observe from (P2) that the null-cline $\dot{v} = 0$ is also a straight line, which passes through the equilibrium:

$$\dot{v} = 0 \quad \Longleftrightarrow \quad w - w_\infty = -\lambda_\varepsilon(v - v_\infty), \qquad \lambda_\varepsilon := \frac{\varepsilon}{1+\varepsilon} < 1,$$

Note that since $\lambda_\varepsilon < 1$, the nullcline $\dot{v} = 0$ is below $p = 0$ for $v \le v_\infty$ and above $p = 0$ for $v \ge v_\infty$. Next, we introduce a line $W_\lambda$ between $\dot{v} = 0$ and $p$ with a slope $\lambda \in (\lambda_\varepsilon, 1)$ to be chosen later:

$$W_\lambda : \quad w - w_\infty = -\lambda(v - v_\infty), \qquad \lambda \in (\lambda_\varepsilon, 1).$$

Similarly, we define on the opposite side of $p = 0$ the line $W_\Lambda$:

$$W_\Lambda : \quad w - w_\infty = -\Lambda(v - v_\infty), \qquad \Lambda := 2 - \lambda > 1.$$

In the following, we denote by $\triangle_\lambda^-$ the open triangle in the phase space $(v, w) \in \mathbb{R}^2_+$, which is defined by the interior between the lines $W_\lambda$, $W_\Lambda$ and $v = 0$. Note that on $\triangle_\lambda^-$ we have $0 < v < v_\infty$ and $w_\infty < w < w_\infty + \Lambda v_\infty$. Analog, the open triangle $\triangle_\lambda^+$ is defined as the interior of the lines $W_\lambda$, $W_\Lambda$ and $w = 0$, i.e. we consider $v_\infty < v < v_\infty + w_\infty/\lambda$ and $0 < w < w_\infty$.

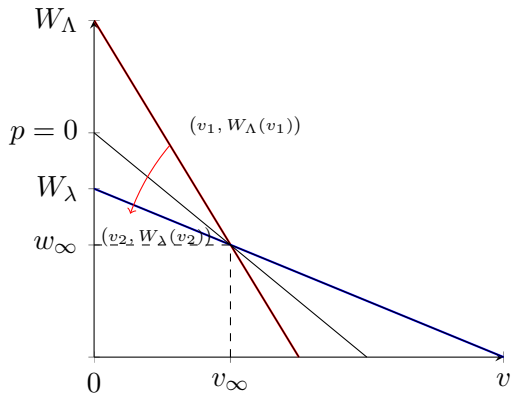


Figure 4: Phase space for the system (P2)

In the following, we shall detail the estimates on the triangle $\triangle_\lambda^-$ for $0 < v < v_\infty$, while the estimates for $\triangle_\lambda^+$ follow analog (e.g. by exchanging the variables $v$ and $w$ and the roles of $\lambda$ and $\Lambda$). We first observe that $w - w_\infty \in (-\lambda(v - v_\infty), -\Lambda(v - v_\infty))$, which implies

$$(1 - \lambda)(v - v_\infty) \le p \le (1 - \Lambda)(v - v_\infty).$$

Moreover, we point out that $\dot v < 0$ and $\dot w < 0$ are strictly negative on $\triangle_\lambda^-$. Hence, whenever a solution trajectory enters $\triangle_\lambda^-$ at some time $t_1$ at a point $(v(t_1), w(t_1)) = (v_1, W_\Lambda(v_1))$ with $v_1 < v_\infty$, then it must leave $\triangle_\lambda^-$ again (after a finite timespan, see Lemma 4 in Appendix A) at a time $t_2$ at a point $(v(t_2), w(t_2)) = (v_2, W_\lambda(v_2))$, for which holds that $0 < v_2 < v_1$.

In order to quantify that all solution trajectories pass through the line of degeneracy $p = 0$ where $\dot H = 0$, we shall prove the $p^2(t)$ is a strictly convex function near $p = 0$ with a positive lower bound for $\ddot p$ within the triangle $\triangle_\lambda^-$ (and $\triangle_\lambda^+$) for $\lambda$ chosen sufficiently close to one, i.e. that $p(t) = 0$ can only occur at discrete points in time.

We begin by calculating

$$\dot p = \dot v + \dot w = d - \varepsilon(v + w)p, \qquad \text{with} \quad d := vw_\infty - wv_\infty.$$

Note that $d = (v - v_\infty)w_\infty - (w - w_\infty)v_\infty$ and on the triangle $\triangle_\lambda^-$, we have

$$\text{on } \triangle_\lambda^- \ : \ d < 0 \quad \text{with} \quad -(v - v_\infty)[w_\infty + \lambda v_\infty] \le |d| \le -(v - v_\infty)[w_\infty + \Lambda v_\infty]. \tag{14}$$

Next,

$$\dot{d} = -\left[(v - v_\infty)v_\infty w + (w - w_\infty)vw_\infty\right] - \varepsilon dp,$$

and

$$\begin{aligned}\ddot{p} = &-\left[(v - v_\infty)v_\infty w + (w - w_\infty)vw_\infty\right] \\ &- 2\varepsilon dp - \varepsilon(v + w)d + \varepsilon^2(v + w)p^2 + \varepsilon^2(v + w)^2 p.\end{aligned}$$

If $p(t_0) = 0$, then

$$p^2(t) = \underbrace{p^2(t_0)}_{=0} + 2\underbrace{p^2(t_0)}_{=0}\dot{p}(t_0)(t - t_0) + 2\left[(\dot{p})^2 + p\ddot{p}\right](\theta)\,\frac{(t - t_0)^2}{2} = \left[(\dot{p})^2 + p\ddot{p}\right](\theta)\,(t - t_0)^2,$$

for some $\theta \in (t, t_0) \subset (t_1, t_2)$. Hence, by using Lemma 3 (see Appendix A) and for $\varepsilon$ sufficiently small

$$\begin{aligned}(\dot{p})^2 + p\ddot{p} &= d^2 - \left[(v - v_\infty)v_\infty w + (w - w_\infty)vw_\infty\right]p + O(\varepsilon) \\ &\ge \kappa(v(\theta) - v_\infty)^2 \ge \kappa(v_1 - v_\infty)^2\end{aligned}$$

for a constant $\kappa > 0$. Now, for any solution trajectory crossing $\triangle_\lambda^-$ between a time interval $(t_1, t_2)$, we estimate

$$\begin{aligned}\int_{t_1}^{t_2} \dot{H} &= -\varepsilon \int_{t_1}^{t_2} p^2(t)\,dt = -\varepsilon \int_{t_1}^{t_2} \left[(\dot{p})^2 + p\ddot{p}\right](\theta)(t - t_0)^2\,dt \\ &\le -\varepsilon\kappa(v_1 - v_\infty)^2 \int_{t_1}^{t_2} (t - t_0)^2\,dt \le -\varepsilon\kappa \int_{t_1}^{t_2} C_1(v(t) - v_\infty)^2\,dt\,\frac{\int_{t_1}^{t_2}(t - t_0)^2\,dt}{t_2 - t_1} \\ &\le -\varepsilon\kappa\, C_1 K \int_{t_1}^{t_2} (v(t) - v_\infty)^2\,dt,\end{aligned}$$

where $C_1 = \frac{(v_1 - v_\infty)^2}{(v_2 - v_\infty)^2} < 1$ since $v_2 < v(t) < v_1$ for all $t \in (t_2, t_1)$ and $K$ is a constant only depending on (a lower bound of) the crossing time $t_2 - t_1$ of all solution trajectory through $\triangle_\lambda^-$ as estimated in Lemma 4 of Appendix A.

Next, we observe that the convexity of the Hamiltonian $H$ together with the decay of the Hamiltonian $H(v(t), w(t)) \le H^0$ for all $t \ge 0$ imply uniform-in-time positive lower and upper

bounds on $v$ and $w$ subject to initial data with finite $H^0 = H(v^0, w^0) < +\infty$. By using this lower and upper bounds, we estimate

$$H(v,w) - H(v_\infty, w_\infty) = v_\infty h\Big(\frac{v}{v_\infty}\Big) + w_\infty h\Big(\frac{w}{w_\infty}\Big) \\ \leq C_2(v_\infty, w_\infty, H^0)\left[(v-v_\infty)^2 + (w-w_\infty)^2\right], \tag{15}$$

where $h(z) = (z-1) - \ln z \geq 0$ is non-negative and convex and $h(z) \leq C_2(z_*, z^*)(z-1)^2$ for $z \in (z_*, z^*)$. Hence, on $\triangle_\lambda^-$, we have $H(v,w) - H(v_\infty, w_\infty) \leq C_3(v-v_\infty)^2$ with a constant $C_3 = C_3(C_2, \lambda)$ and conclude that

$$\int_{t_1}^{t_2} \dot{H} \leq -\varepsilon\kappa C_1 K C_3^{-1} \int_{t_1}^{t_2} H(v,w) - H(v_\infty, w_\infty)\, dt \tag{16}$$

Note that an analog estimate to (16) holds also on $\triangle_\lambda^+$.

Outside of $\triangle_\lambda = \triangle_\lambda^- \cup \triangle_\lambda^+$, there exists a constant $C_\lambda > 0$ such that the estimate $|p|^2 \geq C_\lambda\left[(v-v_\infty)^2 + (w-w_\infty)^2\right]$ holds. Moreover, the uniform lower and upper bounds on $v(t), w(t)$ imply that there exists a positive constant $C_4 = C_4(v_\infty, w_\infty, H^0)$

$$0 < C_4 := \min_{\{(v,w):H(v,w)\leq H^0\}\setminus\triangle_\lambda} \left\{ \frac{[(v-v_\infty) + (w-w_\infty)]^2}{v_\infty h\big(\frac{v}{v_\infty}\big) + w_\infty h\big(\frac{w}{w_\infty}\big)} \right\},$$

which implies $p^2 \geq C_4(H(v,w) - H(v_\infty, w_\infty)$ and

$$\dot{H} \leq -\varepsilon\, C_4(H(v,w) - H(v_\infty, w_\infty)) \qquad \text{outside of} \quad \triangle_\lambda. \tag{17}$$

Estimate (17) proves exponential convergence (of order $\varepsilon$) towards equilibrium first in the relative Hamiltonian distance $(H(v,w) - H(v_\infty, w_\infty))$ as long as a solution trajectory is outside the critical area $\triangle_\lambda$. Consequentially, the reversed estimate (15) (which holds equally true on all points with $H(v,w) \leq H^0$) implies exponential convergence towards equilibrium in the Euclidian distance.

Within the critical area $\triangle_\lambda$, this exponential convergence is hampered by the line of degeneracy where $p = 0$. However, (16) and the lower crossing time estimates in Lemma 4 of Appendix A show that solutions trajectories do not get stuck (or significantly slowed down) within $\triangle_\lambda$. More precisely, since the speed of trajectories outside $\triangle_\lambda$ is bounded above, for any fixed $\lambda < 1$ (sufficiently close to one), all solution trajectories will remain within $\triangle_\lambda$ only a small fraction (let say 10%) of the time spend for one rotation around $(v_\infty, w_\infty)$. Moreover, recall that trajectories can only reach $(v_\infty, w_\infty)$ outside of $\triangle_\lambda$ due to the sign conditions on $\dot{v}$ and $\dot{w}$.

Finally, this small fraction spent within $\triangle_\lambda$ per rotation can not degenerate near $(v_\infty, w_\infty)$, since classical linearisation techniques shows eigenvalues of the form

$$\mu = -\varepsilon\frac{P_0}{2} \pm i\sqrt{(P_0 - M)M + \varepsilon P_0(2M - P_0) - \frac{5}{4}\varepsilon^2 P_0^2} \quad \xrightarrow{\varepsilon\to 0} \quad \pm i\sqrt{v_\infty w_\infty}, \tag{18}$$

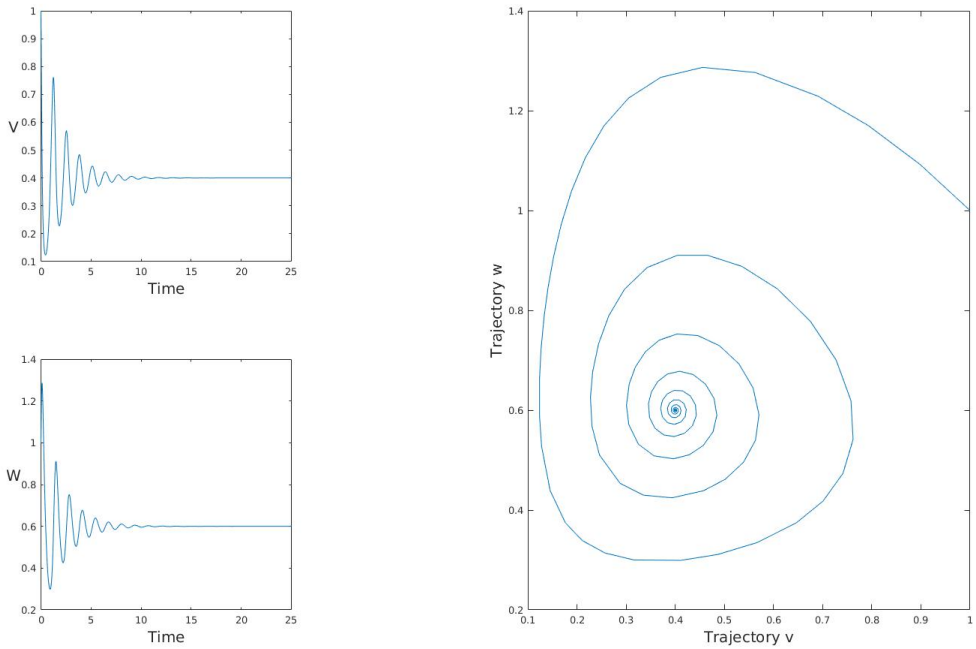


Figure 5: Trajectories of the monomeric concentrations $v$ and $w$ for the two-polymer model for $k = 10$, $a = b = 1$ and $\frac{kM}{1+k} < P_0 < kM$.

where the right hand side values corresponds to the eigenvalues (und thus finite oscillation period) of the zero order Lotka-Volterra system (10).

Altogether, we obtain exponential convergence to equilibrium with a rate $\varepsilon r$ as in (13), where $r$ can be estimated explicitly in terms of the constants in (17) and (16) as well as the crossing times in Lemma 4. ■

### 3.2 Asymptotic expansion for fast monomer-conformer exchange

In the following, we show that system (P2), i.e.

$$\begin{cases} \frac{dv}{dt} = v\left[w_\infty - w\right] - \varepsilon\, v\left[v - v_\infty + w - w_\infty\right], \\ \frac{dw}{dt} = w\left[v - v_\infty\right] - \varepsilon\, w\left[v - v_\infty + w - w_\infty\right]. \end{cases}$$

constitutes a regular perturbation in terms of $\varepsilon$ of the zero order Lotka-Volterra system (10). This is summarised in the following corollary.

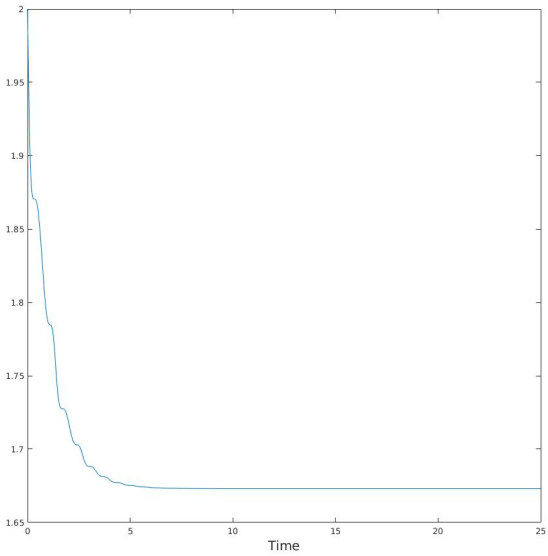


Figure 6: Monotone decay of the Lyapunov functional (12) for the two-polymer model for $k = 10$, $a = b = 1$ and $\frac{kM}{1+k} < P_0 < kM$.

**Corollary 1** (Fast transient oscillations)**.**
*Assume $\varepsilon$ sufficiently small as in the second part of Proposition 1.*

*Then, system* (P2) *is a regular perturbation of the zero order system Lotka-Volterra* (10)*. More precisely, by applying the expansion*

$$v = v_0 + \varepsilon v_1 + O(\varepsilon^2), \qquad \text{and} \qquad w = w_0 + \varepsilon w_1 + O(\varepsilon^2), \tag{19}$$

*the zero order terms $(v_0(t), w_0(t))$ are periodic solutions with period $T > 0$ to the Lotka-Volterra system* (10) *while the first order terms $(v_1(t), w_1(t))$ are solutions to the following non-autonomous linear inhomogeneous system*

$$\begin{pmatrix} \dot{v_1} \\ \dot{w_1} \end{pmatrix} = \underbrace{\begin{pmatrix} w_\infty - w_0 & -v_0 \\ w_0 & v_0 - v_\infty \end{pmatrix}}_{=:A(t)} \cdot \begin{pmatrix} v_1 \\ w_1 \end{pmatrix} - \underbrace{\begin{pmatrix} v_0(v_\infty - v_0 + w_\infty - w_0) \\ w_0(v_\infty - v_0 + w_\infty - w_0) \end{pmatrix}}_{=:g_1(t)}. \tag{20}$$

*Finally, the solutions $(v(t), w(t))$ of system* (P2) *will deviate $O(\varepsilon)$ far from the $T$-periodic zero order solution $(v_0(t), w_0(t))$ on a time interval of size $O(T)$ and hence undergo $O(1/\varepsilon)$ many oscillations before converging to $(v_\infty, w_\infty)$ as proven in Proposition 1.*

**Proof.** Global existence of the first order terms $(v_1(t), w_1(t))$ follows from classical ODE theory. In fact, since $(v_0(t), w_0(t))$ is periodic with period $T$, also $A(t)$ and $g_1(t)$ are $T$-periodic and

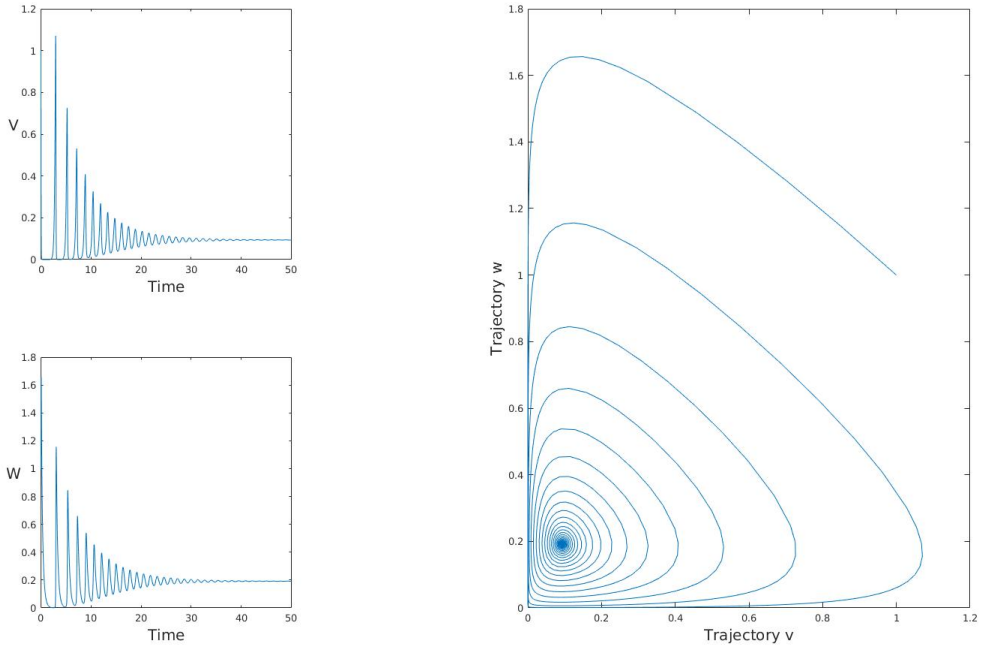


Figure 7: Trajectories of the monomeric concentrations $v$ and $w$ for the two-polymer model for $k = 35$, $a = b = 1$ and $\frac{kM}{1+k} < P_0 < kM$.

Floquet theory implies that solutions to (20) are $T$-periodic if and only if one is not a Floquet multiplier, i.e. an eigenvalue of the associated monodromy matrix, see e.g. [25, Chapter 3.6]. However, the Lyapunov structure and the exponential decay of Proposition 1 imply that system (20) has to be entirely unstable and that both Floquet multipliers have to be larger than one.

Moreover, all higher order expansion terms $(v_n(t), w_n(t))$ for $n \geq 2$ satisfy analog systems to (20) with the same non-autonomous system matrix $A(t)$ and similar inhomogeneities $g_n(t)$ only depending on the previously determined asymptotic expansion terms $(v_0, w_0), \ldots, (v_{n-1}, w_{n-1})$.

Hence, (19) constitutes a regular asymptotic expansion of the solution $(v, w)$ up to arbitrarily high order. In particular, this implies that the change of the full solution $(v, w)$ compared to the zero order approximation $(v_0, w_0)$ over one period is of order $\varepsilon$ and that $(v, w)$ will undergo order $1/\varepsilon$ many oscillations before finally converging to the equilibrium $(v_\infty, w_\infty)$. ■

Figures 5, 6 and 7 illustrate Corollary 1 for value $k = 10$ and $k = 35$. Clearly, the number of oscillations increases with $k$, while all other parameters being left unchanged. Moreover, Figure 6 shows the monotone decay of the Lyapunov functional in the case $k = 10$: we observe a general exponential decay despite the successive plateaus, which occur when solutions cross the lines of

degeneracy $p = 0$.

# 4 The $n-$polymer model

Let us now turn to the system (6) in the case where $3 \leq n < \infty$.

## 4.1 Steady states analysis

System (6) with finite $n$ features both boundary steady states (BSS), where at least one concentration is zero, and positive steady state (PSS), where all concentrations are strictly positive.

Let us first introduce several parametric regions – graphically illustrated in Figure 8– which will defining the stability or instability regions of the boundary steady states (BSS).

$$n + \frac{b_n}{k} \leq \frac{M_{tot}}{P_0} \qquad \text{(region with horizontal green stripes in Fig. 8)}, \tag{21}$$

$$n < \frac{M_{tot}}{P_0} < n + \frac{b_n}{k} \qquad \text{(light blue region in Fig. 8)}, \tag{22}$$

$$\frac{M_{tot}}{P_0} \leq 1 + \frac{a_1}{k} \qquad \text{(grey diagonally hatched region in Fig. 8)}. \tag{23}$$

**Proposition 1** (Nonnegative Steady States)**.**
*Let $a_i > 0$, $b_{i+1} > 0$ for $1 \leq i \leq n-1$, let $v_0$, $w_0 > 0$ and $P_0 > 0$, $M_{tot} \geq v_0 + w_0 + P_0 > 0$. Then,*

*1. there exists three kinds of boundary steady states (BBS):*

*(BSSa) There exist unstable BSSs: $\bar{v} = \bar{w} = 0$ and $(\bar{c}_i)_{1 \leq i \leq n}$ satisfies $\sum_{i=1}^{n} \bar{c}_i = P_0$, $\sum_{i=1}^{n} i\bar{c}_i = M_{tot}$.*

*(BSSb) There exists a BSS: $\bar{v} = M_{tot} - P_0 > 0$, $\bar{w} = 0$, $\bar{c}_1 = P_0$, $\bar{c}_i = 0$ for $2 \leq i \leq n$. This BSS is locally asymptotically stable under Assumption (23) (grey diagonally hatched) and unstable elsewhere.*

*(BSSc) Under the additional assumption $\frac{M_{tot}}{P_0} > n$, there exists another BSS: $\bar{v} = 0$, $\bar{w} = M_{tot} - nP_0 > 0$, $(\bar{c}_i)_{1 \leq i \leq n-1} = 0$ and $c_n = P_0$. This BSS is locally asymptotically stable under Assumption (21) (green horizontal lines) and otherwise unstable, which corresponds to Assumption (22) (light blue zone). Note that (BSSc) disappears in the infinite system (6), see Section 5.2.*

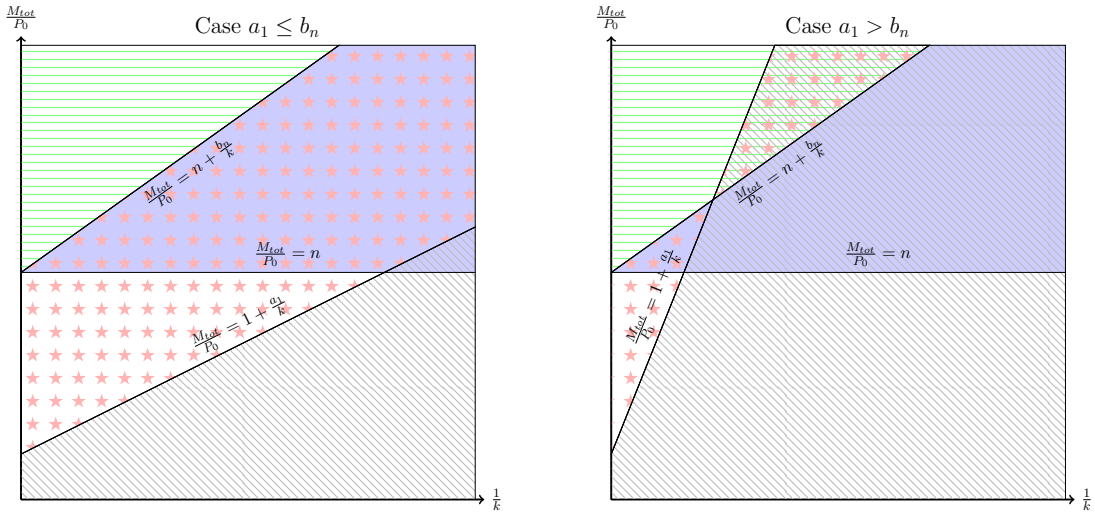


Figure 8: Stability regions of the SSs of the finite system (6) in the $\frac{1}{k}$-$\frac{M_{tot}}{P_0}$ parametric space: (BSSa) are always unstable. Grey diagonally hatched zone $\iff$ (23) $\iff$ asymptotically stable (BSSb), which is unstable elsewhere. Green horizontal lines $\iff$ (21) $\iff$ asymptotically stable (BSSc). Light blue zone $\iff$ (22) $\iff$ unstable (BSSc). Zone with red stars $\iff$ existence of at least one PSS (in case $a_1 > b_n$ coexisting with a stable (BSSb) in the diagonally hatched region; otherwise coexisting only unstable BSSs.)

2. *There exists (at least one) positive steady state (PSS)* $(\bar{v}, \bar{w}, \bar{c}_i)_{1\le i\le n}$ *provided that the polynomial* $P(z)$ *defined as*

$$P(z) := \left[\frac{a_1}{k} + 1 - \frac{M_{tot}}{P_0}\right] + \sum_{i=2}^{n-1}\left[\left(\frac{a_i}{k} + i - \frac{M_{tot}}{P_0} + \frac{b_i}{k}\right)\prod_{j=0}^{i-1}\frac{a_j}{b_{j+1}}\right] z^{i-1} + \left[\left(n - \frac{M_{tot}}{P_0} + \frac{b_n}{k}\right)\prod_{j=0}^{n-1}\frac{a_j}{b_{j+1}}\right] z^{n-1}. \quad (24)$$

*has a root* $\bar{z} > 0$. *Given* $z > 0$, *we have*

$$\begin{aligned} \bar{v} &= \bar{c}_1 \sum_{i=1}^{n-1} \frac{a_i}{k} \bar{z}^{i-1} \prod_{j=0}^{i-1} \frac{a_j}{b_{j+1}}, & \bar{w} &= \bar{c}_1 \sum_{i=1}^{n-1} \frac{a_i}{k} \bar{z}^{i} \prod_{j=0}^{i-1} \frac{a_j}{b_{j+1}}, \\ \bar{c}_1 &= \frac{P_0}{\sum_{i=1}^{n} \bar{z}^{i-1} \prod_{j=0}^{i-1} \frac{a_j}{b_{j+1}}}, & \bar{c}_i &= \bar{z}^{i-1} \prod_{j=0}^{i-1} \frac{a_j}{b_{j+1}} \bar{c}_1, \quad 2 \le i \le n. \end{aligned} \quad (25)$$

*If all BSSs are unstable, then there exists at least one positive steady state. Moreover, if the*

*sequences $(a_i)$, $(b_i)$ are nondecreasing and $\frac{M_{tot}}{P_0} \leq n + \frac{b_n}{k}$, the positive steady state is unique.*

**Remark 1.** *The existence of positive roots of the polynomial $P$ can be analysed in more detail in the case of constant polymerisation coefficients, see Proposition 2 below. Also, the computation of those roots can be done numerically. While the linear stability of the BSSs can be calculated explicitly, the stability of the PSS constitutes a difficult problem, which can be explicitly confirmed in the two-polymer model, see* (18)*, but seems otherwise only possible by numerical calculations.*

**Proof.** For simplicity of notations, we drop the $\bar{\cdot}$ in what follows, and postpone the proofs of stability to Appendix B. The steady states of the system (6) satisfy the following relations:

$$\begin{cases} -kvw + v\sum_{i=2}^{n} b_i c_i \ = 0, & -w\sum_{i=1}^{n-1} a_i c_i + kvw \ = 0, \qquad J_1 = \ldots = J_{n-1} \ = 0, \\ \sum_{i=1}^{n} c_i = P_0, & v + w + \sum_{i=1}^{n} i c_i = \ M_{tot}. \end{cases} \tag{26}$$

1. First, we discuss the existence of BSSs, where at least one of the two monomeric species vanishes:

   (a) If $w = v = 0$, then any distribution $(c_i)$ such that $\sum_{i=1}^{n} c_i = P_0$ and $\sum_{i=1}^{n} i c_i = M_{tot}$ is a steady state solution.

   (b) If $w = 0$ and $v \neq 0$, then by the first equation we have $v\sum_{i=2}^{n} b c_i = 0$, hence $c_i = 0$ for $i \geq 2$, so that $c_1 = P_0$ and $v$ is such that $v + c_1 = M_{tot}$.

   (c) If $v = 0$ and $w \neq 0$, then by the second equation we have $w\sum_{i=1}^{n-1} a c_i = 0$, hence $c_i = 0$ for $i \leq n-1$, so that $c_n = P_0$ and $w$ is such that $w + n c_n = M_{tot}$.

2. Let us now consider $v > 0$ and $w > 0$. Since $J_i = 0$, we have by immediate recursion

$$c_i = \frac{a_{i-1} w}{b_i v} c_{i-1} = \cdots = \left( \prod_{j=0}^{i-1} \alpha_j \right) z^{i-1} c_1, \qquad \forall\ 2 \leq i \leq n,$$

   where $\alpha_i = \frac{a_i}{b_{i+1}}$, $\alpha_0 = 1$ and $z = \frac{w}{v}$. Inserting this identity into (26), yields

$$kv = c_1 \sum_{i=1}^{n-1} a_i z^{i-1} \prod_{j=0}^{i-1} \alpha_j, \qquad P_0 = c_1 \sum_{i=1}^{n} z^{i-1} \prod_{j=0}^{i-1} \alpha_j,$$

and

$$M_{tot} = v(1+z) + c_1 \sum_{i=1}^{n} i z^{i-1} \prod_{j=0}^{i-1} \alpha_j = c_1 \Big( \sum_{i=1}^{n-1} \frac{a_i}{k} z^{i-1}(1+z) \prod_{j=0}^{i-1} \alpha_j + \sum_{i=1}^{n} i z^{i-1} \prod_{j=0}^{i-1} \alpha_j \Big)$$
$$= c_1 \Big( \sum_{i=1}^{n-1} \frac{a_i}{k} z^{i-1} \prod_{j=0}^{i-1} \alpha_j + \sum_{i=2}^{n} \frac{a_{i-1}}{k} z^{i-1} \prod_{j=0}^{i-2} \alpha_j + \sum_{i=1}^{n} i z^{i-1} \prod_{j=0}^{i-1} \alpha_j \Big)$$
$$= c_1 \Big( \frac{a_1}{k} + 1 + \sum_{i=2}^{n-1} \Big( (\frac{a_i}{k} + i)\alpha_{i-1} + \frac{a_{i-1}}{k} \Big) \prod_{j=0}^{i-2} \alpha_j z^{i-1} + \Big( \frac{a_{n-1}}{k} + n\alpha_{n-1} \Big) \prod_{j=0}^{n-2} \alpha_j z^{n-1} \Big).$$

We deduce

$$\frac{M_{tot}}{c_1} = \frac{M_{tot}}{P_0} \sum_{i=1}^{n} z^{i-1} \prod_{j=0}^{i-1} \alpha_j$$
$$= \frac{a_1}{k} + 1 + \sum_{i=2}^{n-1} \Big( (\frac{a_i}{k} + i)\alpha_{i-1} + \frac{a_{i-1}}{k} \Big) \prod_{j=0}^{i-2} \alpha_j z^{i-1} + \Big( \frac{a_{n-1}}{k} + n\alpha_{n-1} \Big) \prod_{j=0}^{n-2} \alpha_j z^{n-1},$$

and finally

$$P(z) = \Big[ \frac{a_1}{k} + 1 - \frac{M_{tot}}{P_0} \Big] + \sum_{i=2}^{n-1} \Big[ \Big( \Big( \frac{a_i}{k} + i - \frac{M_{tot}}{P_0} \Big) \alpha_{i-1} + \frac{a_{i-1}}{k} \Big) \prod_{j=0}^{i-2} \alpha_j \Big] z^{i-1}$$
$$+ \Big[ \Big( \Big( n - \frac{M_{tot}}{P_0} \Big) \alpha_{n-1} + \frac{a_{n-1}}{k} \Big) \prod_{j=0}^{n-2} \alpha_j \Big] z^{n-1} = 0.$$

If $1 + \frac{a_1}{k} < \frac{M_{tot}}{P_0} < n + \frac{b_n}{k}$, we have $P(0) < 0$ and $P(+\infty) = +\infty$, so that $P$ admits at least one positive root.

■

*Discussion and biological interpretation:* The steady state analysis of Proposition 1 revealed different parametric regions. A key quantity appears to be the ratio $\frac{M_{tot}}{P_0}$, which is easily interpreted as the sum of the average size of polymers plus the ratio representing the relative numbers of monomers to polymers, i.e.

$$\frac{M_{tot}}{P_0} = \frac{\sum i c_i}{P_0} + \frac{v+w}{P_0}.$$

Figure 8 illustrates Proposition 1. The extrem case $\frac{\sum i c_i}{P_0} = n$ is equivalent to $c_n = P_0$. Therefore, the zones $\frac{M_{tot}}{P_0} > n$ (green horizontal lines and light blue zone) can be interpreted either as

situations with a high amount of very large polymers close to the maximal size $n$ or as situations with a large amount of the monomeric species $v$ and $w$ (compared to $P_0$). From a biological view, both those situations seem very unlikely. Hence (BSSc) and its stability is conjectured to have little biological relevance. Moreover, (BSSc) will disappear in the limit $n \to \infty$, see Section 5.

The biologically more realistic zone $\frac{M_{tot}}{P_0} < n$ is divided into only two parts: either Assumption (23) is fulfilled, and (BSSb) is locally asymptotically stable (grey diagonally hatched region), or all BSSs are unstable whereas there exists a PSS (red stars zone). Assumption (23) has a direct interpretation that there is not enough initial mass to ignite the polymerisation hierarchy in the sense that all polymers depolymerise into the species $\mathcal{C}_1$. Indeed (BSSb), which is stable under Assumption (23), features $\bar{c}_1 = P_0$ while $\bar{c}_i = 0$ for $2 \leq i \leq n$. Conversely, in the red star region, the system features a PSS (which is conjectured to be stable). In the dichotomy of stable (BSSb) versus existence of a PSS, the convergence to (BSSb) could be considered as non-proliferation of a disease in a more specific prionic model while otherwise a prionic assembly gets established in terms of the PSS.

From a more conceptional modelling viewpoint, the $n$-polymer model couples the bi-monomeric equations for $v$ and $w$ to a finite range of polymers of sizes 1 to $n$, which are considered as biologically "active", *i.e.* they interact with the monomeric species. More than the two-polymer model, the $n$-polymer model with increasing $n$ describes the interaction of the bi-monomeric dynamics for $v$ and $w$ with a larger and larger hierarchy of polymerising and depolymerising polymers. The nonlinear feedback from the polymer-hierarchy is sufficient to introduce sustained oscillatory behaviour already in the two-polymer model, but it can be hypothesised that with larger $n$ the dynamical interplay between monomer species and polymer hierarchy becomes more intricate, cf. Figure 12 below.

In any case, model system (6) should be understood as a prototypical building block of more realistic and prion specific models. In the experiment illustrated in Figure 1, for instance, oscillations appear only during a specific time range; other reactions may have occured before, giving progressively rise to polymers belonging to the "active" range of the $n$-polymer model. Moreover, from a mathematical perspective, the $n$-polymer model is an interesting intermediate before turning to the infinite system.

#### 4.1.1 Case of constant polymerisation coefficients

If the reaction coefficients are constant, *i.e.* the polymerisation/depolymerisation speed is the same for all polymers regardless of their size, the polynomial $P$ defined in (24) (characterising PSSs) takes a simpler expression, which is stated in the following corollary.

**Corollary 2** (Positive steady states in the constant coefficients case)**.**
*Let $k$, $b$, $a$, $P_0$ and $M_{tot}$ be positive real constants. Let $a_i = a$ and $b_{i+1} = b$ for $1 \leq i \leq n$ in System* (6)*. Let $n \geq 3$. Then,*

1. *if the initial conditions and parameters satisfy the condition*

$$\frac{M_{tot}}{P_0} = \left(\frac{a}{k} + \frac{b}{k}\right)\frac{n-1}{n} + \frac{n+1}{2}, \tag{27}$$

*there exists a unique positive steady state (PSS) to system* (6)*, which is defined by*

$$\bar{c}_i := \frac{P_0}{n} \qquad \forall\, 1 \le i \le n, \qquad \bar{v} = \frac{a}{k}P_0, \qquad \bar{w} = \frac{b}{k}P_0.$$

2. *If* (27) *is not satisfied, then the PSSs of the system* (6) *are given by* $(\gamma, \bar{v}, \bar{w}, \bar{c}_1)$ *where* $\gamma \neq 1$ *is a root of the following polynomial*

$$Q(\gamma) := P(\frac{b}{a}\gamma) = \Big(\frac{a}{k} - \frac{M_{tot}}{P_0} + 1\Big) + \sum_{k=1}^{n-2}\Big(\frac{a}{k} + \frac{b}{k} - \frac{M_{tot}}{P_0} + k + 1\Big)\gamma^k + \Big(\frac{b}{k} - \frac{M_{tot}}{P_0} + n\Big)\gamma^{n-1}, \tag{28}$$

*and* $(\bar{c}_1, \bar{v}, \bar{w})$ *are defined from* $\gamma$ *by*

$$\bar{c}_1 := P_0\frac{1-\gamma}{1-\gamma^n}, \qquad \bar{v} := \frac{a}{k}P_0\frac{1-\gamma^{n-1}}{1-\gamma^n}, \qquad \bar{w} := \frac{b}{k}P_0\frac{\gamma-\gamma^n}{1-\gamma^n}. \tag{29}$$

**Remark 2.** *The relation* (27) *shall never be satisfied in practice, but it may be* roughly *satisfied in the sense that if* $n$ *is large, it corresponds to the case where the average size of the polymers is initially taken around* $\frac{n}{2}$*. We shall see later (Proposition 3) how this average size is related to the cases* $\gamma < 1$ *or* $\gamma > 1$*.*

**Proof.** We apply Proposition 1 and notice that $P(z) = Q(\gamma)$ with $\gamma = \frac{a}{b}z$ and $Q$ defined by (28). We then distinguish according to $\gamma = 1$ or $\gamma \neq 1$.

1. For $\gamma = 1$, we have

$$\begin{aligned} Q(1) &= \frac{a}{k} - \frac{M_{tot}}{P_0} + 1 + (n-2)\Big(\frac{a}{k} + \frac{b}{k} - \frac{M_{tot}}{P_0} + 1\Big) + \frac{(n-1)(n-2)}{2} - \frac{M_{tot}}{P_0} + \frac{b}{k} + n \\ &= (n-1)\Big(\frac{a}{k} + \frac{b}{k} + \frac{n-2}{2} + 1\Big) - n\frac{M_{tot}}{P_0} + n, \end{aligned} \tag{30}$$

   so that $Q(\gamma) = 0$ *iff* the relation (27) is satisfied, and the value for $c_i$, $v$ and $w$ immediately follow from (25).

2. If $\gamma \neq 1$, we obtain (29) directly from (25).

■

For the existence of PSS, we study roots of the polynomial $Q$ by applying Descartes' rule.

**Lemma 1** (Descartes' rule of signs [14])**.**
*Given a univariate real polynomial $P$, the number of positive real roots of $P$ is bounded by the number of sign variations of the ordered (by exponent) sequence of the coefficients of $P$.*

The following Proposition characterises different cases, leading to zero, one or two positive steady states.

**Proposition 2** (Existence and number of PSSs of system (6) with constant coefficients)**.**
*Consider system* (6) *with constant polymerisation/depolymerisation coefficients $a$, $b$ under the assumptions of Corollary 2. Assume that* (27) *is not satisfied. Then, we have the following cases.*

1. *If one of the following assumptions is satisfied:*

$$\frac{M_{tot}}{P_0} < \min(1 + \frac{a}{k}, n + \frac{b}{k}), \tag{31}$$

$$\frac{M_{tot}}{P_0} > \max(n + \frac{b}{k}, n + \frac{b}{k} + \frac{a}{k} - 1), \tag{32}$$

   *then, system* (6) *with constant coefficients has no PSS.*

2. *If either*

$$1 + \frac{a}{k} < \frac{M_{tot}}{P_0} < n + \frac{b}{k}, \tag{33}$$

   *or*

$$n + \frac{b}{k} < \frac{M_{tot}}{P_0} < 1 + \frac{a}{k}, \tag{34}$$

   *holds, then system* (6) *with constant coefficients has a unique PSS.*

3. *If*

$$\max(\frac{b}{k} + n, \frac{a}{k} + 1) < \frac{M_{tot}}{P_0} < n + \frac{b}{k} + \frac{a}{k} - 1, \tag{35}$$

   *holds, then system* (6) *with constant coefficients has at most two PSSs.*

**Proof.**Using the results of Corollary 2, we look for roots of the polynomial $Q(\gamma) = \sum_{k=0}^{n-1} u_k \gamma^k$, where

$$u_0 = \frac{a}{k} - \frac{M_{tot}}{P_0} + 1, \qquad u_k = \frac{a}{k} + \frac{b}{k} - \frac{M_{tot}}{P_0} + k + 1 = u_0 + \frac{b}{k} + k, \qquad u_{n-1} = \frac{b}{k} - \frac{M_{tot}}{P_0} + n.$$

and we apply the Descartes' rule. We notice that $(u_k)$ is strictly increasing in $k$ for $0 \leq k \leq n-2$, and $u_{n-1} = u_{n-2} - \frac{a}{k} + 1$.

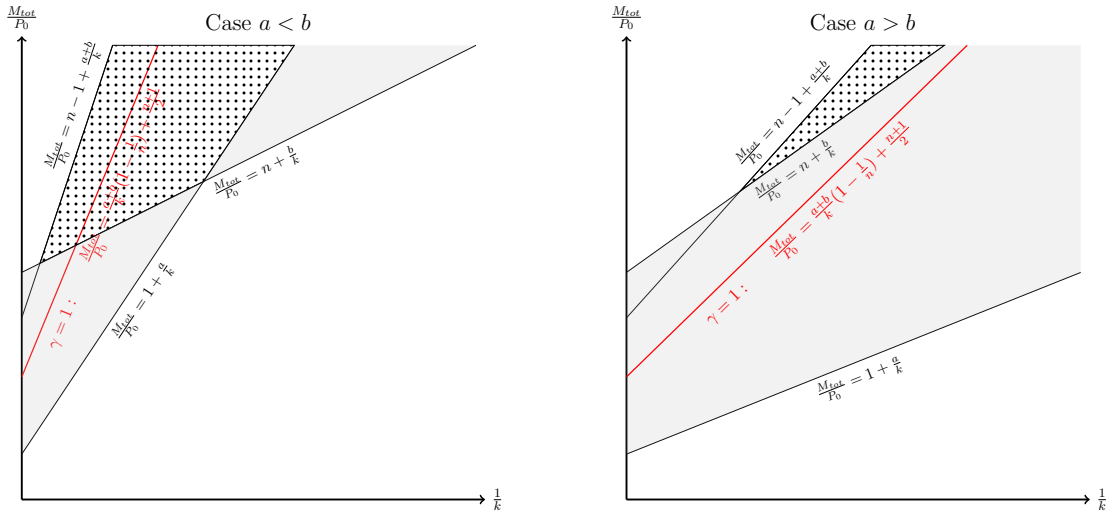


Figure 9: Zones with zero (white), one (light grey) or two (dotted domain) PSSs. In red is the line of assumption (27): above we have $\gamma > 1$, below $\gamma < 1$.

1. If $u_0 > 0$ and $u_{n-1} > 0$, *i.e.* if assumption (31) is satisfied, then, all coefficients are positive. If $u_{n-2} < 0$ and $u_{n-1} < 0$, *i.e.* if assumption (32) is satisfied, then, all coefficients are negative. In both cases, there exists no PSS.

2. If $u_0 < 0$ and $u_{n-1} > 0$, *i.e.* under assumption (33), or if $u_0 > 0$ and $u_{n-1} < 0$, *i.e.* assumption (34), there is exactly one change of sign in the coefficients. In these cases, there exists at most one PSS. In fact, there exists exactly one PSS, because $P(0) = u_0$ and $P(z) \sim u_{n-1} z^{n-1}$ as $z \to \infty$ are of opposite sign.

3. If $u_0 < 0$, $u_{n-2} > 0$ and $u_{n-1} < 0$, *i.e.* under assumption (35), there are two changes of signs in the coefficients, so that there exist at most two PSSs.

■

*Discussion and biological interpretation:* The conditions (31)-(35) are summarised in Figure 9: The grey region is the region where assumptions (33) and (34) are satisfied, i.e. there is a unique PSS. The region with dots corresponds to assumption (35), where there exist at most two PSSs. The white region in the figure corresponds to assumptions (31) and (32) with no PSS. As in the general coefficient case, we see that the zone where there is at least one steady state corresponds to the intermediate zone, where $\frac{M_{tot}}{P_0}$ is neither "small" nor "large" compared to the reaction parameters. Moreover, more than one PSS can only occur in the biologically unrealistic region where $\frac{M_{tot}}{P_0} > n$.

In the case of a unique PSS, let us now study the respective values of $\gamma \gtreqless 1$. This is of key importance, since if $\gamma \geq 1$, then the corresponding PSS has no finite limit as $n \to \infty$.

**Corollary 3** (Values of the root $\gamma$)**.**
*Let the assumptions of Proposition 2 be satisfied and assume moreover inequality* (33)*. Let $\gamma$ be the unique positive root of the polynomial $Q$. Then,*

- *if* $\frac{M_{tot}}{P_0} = \left(\frac{a}{k} + \frac{b}{k}\right)\frac{n-1}{n} + \frac{n+1}{2}$*, we have* $\gamma = 1$*,*
- *if* $\frac{M_{tot}}{P_0} > \left(\frac{a}{k} + \frac{b}{k}\right)\frac{n-1}{n} + \frac{n+1}{2}$*, we have* $\gamma > 1$*,*
- *if* $\frac{M_{tot}}{P_0} < \left(\frac{a}{k} + \frac{b}{k}\right)\frac{n-1}{n} + \frac{n+1}{2}$*, we have* $\gamma < 1$*.*

**Proof.** Under Assumption (33), $Q(0) < 0$ and $Q(\infty) > 0$, so that $\gamma > 1$ iff $Q(1) < 0$. We have already calculated $Q(1)$ in (30), from which the results follows immediately. ■

**Remark 3.** *Letting $n$ tend to infinity while keeping $M_{tot}$ and $P_0$ finite ensures $\gamma < 1$: Hence, the steady state $c_i = c_1\gamma^{i-1}$ defines a converging series and thus a possible steady state for the infinite system. Note that that the assumption of constant polymerisation coefficients prevents gelation (as for the classical Becker-Döring system).*

### 4.2 Simulation results and discussion

Experiments can either measure the total polymerised mass $M_1(t)$ (by Thioflavine T, see e.g. [29]) or the second moment $M_2(t)$ (by Static Light Scattering, see e.g. [23]) defined by

$$M_1 := \sum_{i=1}^{n} ic_i = M_{tot} - v - w, \qquad M_2 := \sum_{i=1}^{n} i^2 c_i(t). \tag{36}$$

The following numerical simulations exemplify the dynamical behaviour of system (6) in two biologically plausible cases: Figures 10, 11 and 12 illustrate damped oscillations converging to a positive steady state (PSS) under Assumption (33) while Figure 13 shows convergence to (BSSb) (recall $\bar{w} = 0$ and $\bar{c}_1 = P_0$) under Assumption (23).

Figure 10: The size distribution of the polymers (right image), initially taken as a sharp Gaussian, oscillates in the sense that the Gaussian moves from left to right and right to left periodically in its entirety while progressively diffusing. Figure 11: For initial states very close to the steady state, the oscillations remain numerous, though of smaller amplitude. Figure 12: An example concerning the influence of the initial average size of the polymers and of the total number of polymers $n$ shows that smaller initial average size implies stronger damping of the oscillations. This supports an intuition that the role played by $k$ in the two-polymer model might be here played by the average size of the polymers, which is about $\frac{n}{2}$ in this example.

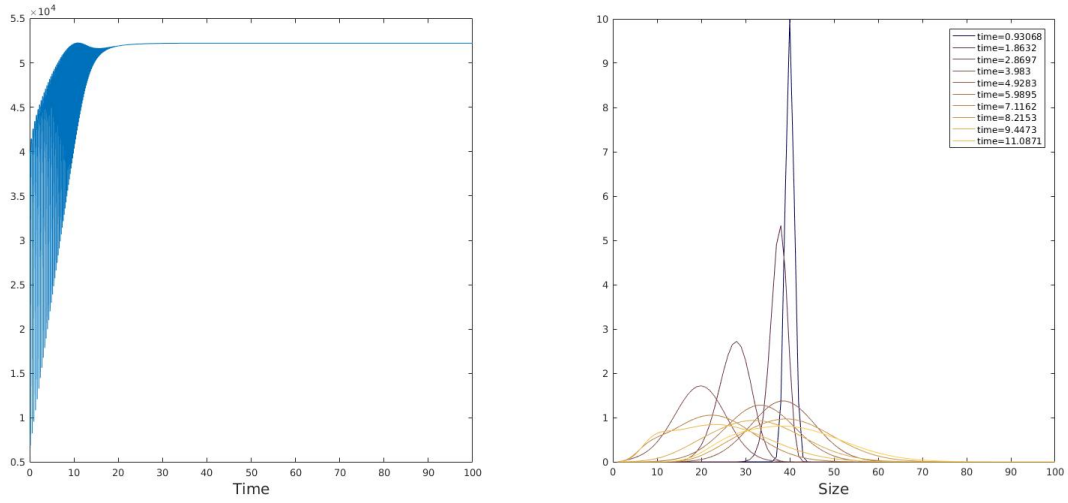


Figure 10: Numerical simulation of convergence to (PSS) as in Proposition 1: $M_2(t)$ defined by (1) (left image) and evolution of the size distribution (right images). The parameters are $n = 100$, $k = 1.1$, $a = 1.5$, $b = 2$ and Assumption (33): $1 + \frac{a}{k} < \frac{M_{tot}}{P_0} < n + \frac{b}{k}$ .

# 5 The infinite system

Let us now turn to the infinite system (6) with $n = \infty$, where no restriction is imposed on the maximal size of a fibril. Infinite size systems like the classical Becker-Döring model or the Prion model [19, 23] are considered the most natural way to model such aggregation processes [5]. In this section, we first present a well-posedness result and, secondly a study of all steady states. Finally, we point out two interesting links of the infinite model with constant respectively linear polymerisation coefficients to Lotka-Volterra systems.

## 5.1 Well-posedness

We introduce the Banach sequence spaces

$$\ell_1^1 = \{y = (y_i) \ : \ \|y\| < \infty\}, \qquad \|y\| = \sum_{i=1}^{\infty} i|y_i|.$$

and

$$\mathcal{X} = \{x = (v, w, c) = (v, w, c_1, c_2, \ldots) \ : \ \|x\|_{\mathcal{X}} < \infty\}, \qquad \|x\|_{\mathcal{X}} = |v| + |w| + \|c\|.$$

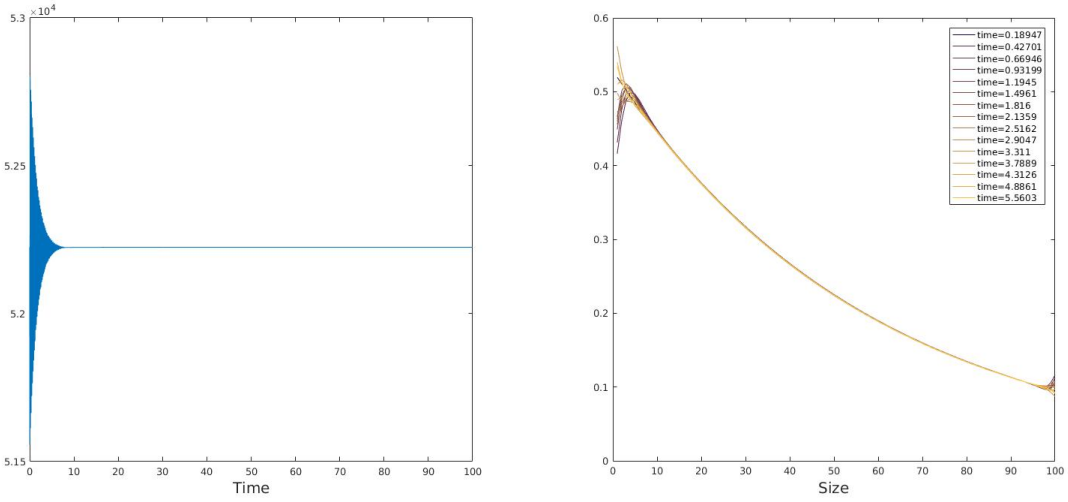


Figure 11: Numerical simulation of convergence to (PSS) as in Proposition 1: $M_2$ defined by (1) (left images) and time evolution of the size distribution (right image). The initial condition is the very (numerical) PSS, but $\bar{v}$ and $\bar{w}$ are perturbed away by a constant of order $10^{-1}$ of their equilibrium values. The parameters are $n = 100$, $k = 1.1$, $a = 1.5$, $b = 2$ and Assumption (33): $1 + \frac{a}{k} < \frac{M_{tot}}{P_0} < n + \frac{b}{k}$.

**Definition 1.** *Let $0 < T \leq \infty$ and $c = (c_i)$. A nonnegative solution $x = (v, w, c)$ of (6) with $n = \infty$ on $[0, T)$ is a function $x : [0, T) \to \mathcal{X}$ such that*

1. *$x(t) \geq 0$ for all $t \in [0; T)$, i.e. $v(t) \geq 0$, $w(t) \geq 0$, $c_i(t) \geq 0$ for each $i$,*
2. *$v, w : [0, T) \to \mathbb{R}$ and $c_i : [0, T) \to \mathbb{R}$ for all $i \geq 1$ are continuous with $\sup_{t\in[0,T)} \|x(t)\|_{\mathcal{X}} < \infty$,*
3. *$\int_0^t \sum_{i=1}^{\infty} a_i c_i(s) ds < \infty$, $\int_0^t \sum_{i=2}^{\infty} b_i c_i(s) ds < \infty$ for all $t \in [0, T)$ and*
4. *$v$, $w$ and $c$ satisfy for all $t \in [0, T)$*

$$\begin{cases} v(t) = v_0 + \int_0^t \left( -kv(s)w(s) + v(s) \sum_{i=2}^{\infty} b_i c_i(s) \right) ds, \\ w(t) = w_0 + \int_0^t \left( -w(s) \sum_{i=1}^{\infty} a_i c_i(s) + kv(s)w(s) \right) ds, \\ c_i(t) = c_i^0 + \int_0^t \Big( J_{i-1}(s) - J_i(s) \Big) ds, \quad i \geq 1, \ J_0 = 0. \end{cases} \tag{37}$$

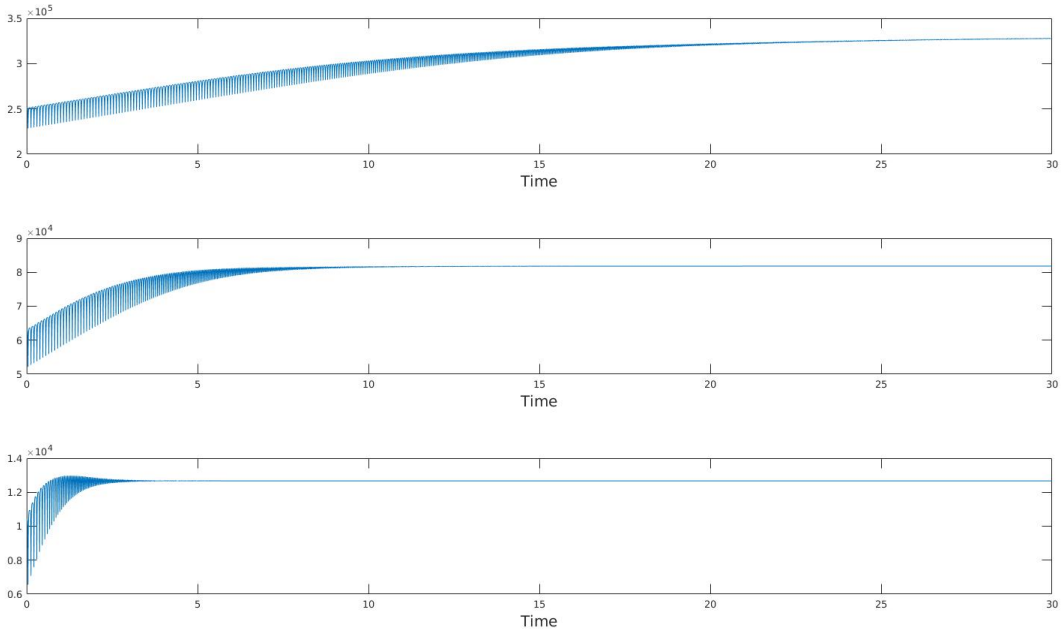


Figure 12: Numerical simulation of convergence to (PSS) as in Proposition 1: $M_2$ defined by (1) and its sensitivity to the number of polymers. The number of polymers are 100 (up), 50 (middle) and 20 (bottom). The initial size distributions are centered on $\frac{n}{2}$. The parameters are $k = 10$, $a = 1.5$, $b = 2$ and Assumption (33): $1 + \frac{a}{k} < \frac{M_{tot}}{P_0} < n + \frac{b}{k}$.

**Lemma 2** (Well-posedness of the finite dimensional system)**.**
*For all $n \in \mathbb{N}$, system (6) has a unique nonnegative solution $v(t) \geq 0$, $w(t) \geq 0$, $c_i(t) \geq 0$ for $t \geq 0$ and all $1 \leq i \leq n$ satisfying*

$$v(t) + w(t) + \sum_{i=1}^{n} i c_i(t) = v_0 + w_0 + \sum_{i=1}^{n} i c_i^0, \qquad \sum_{i=1}^{n} c_i(t) = \sum_{i=1}^{n} c_i^0, \quad \forall t \geq 0.$$

**Theorem 2** (Well-posedness of the infinite dimensional system)**.**
*Let $T > 0$ be arbitrary and consider $x_0 = (v_0, w_0, c_0)$ satisfy $\|x_0\|_{\mathcal{X}} < \infty$. Assume*

$$a_i = O(i), \qquad b_{i+1} = O(i+1), \qquad \forall\, i \geq 1.$$

*Then, system (6) with $n = \infty$ has a nonnegative solution for $t \in [0, T)$ with $v(t) \geq 0$, $w(t) \geq 0$,*

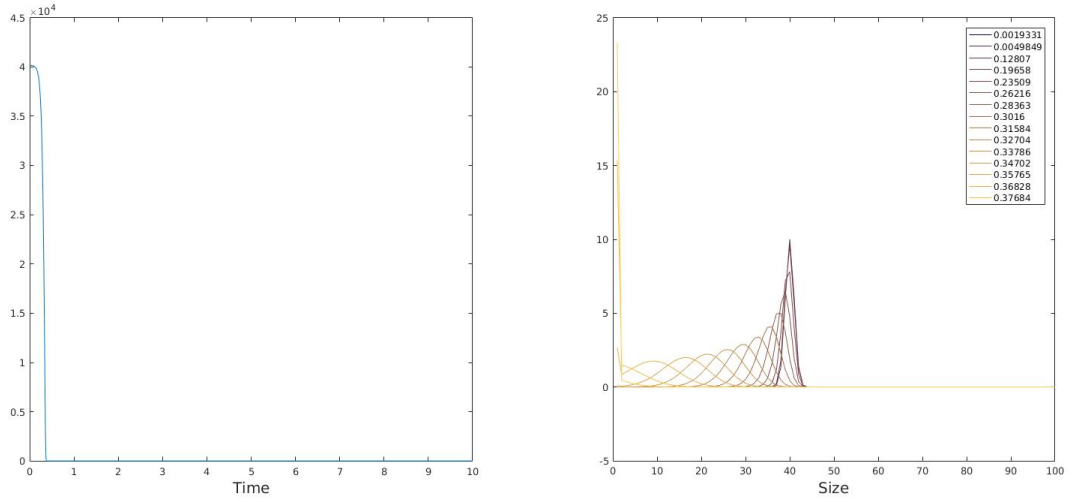


Figure 13: Numerical simulation of convergence to (BSSb) as in Proposition 1: $M_2$ defined by (1) (left images) and time evolution of the size distribution (right image). The initial size distribution is centred around the size 40. The parameters are $n = 100$, $k = 2$, $a = 80$, $b = 1$ and $\frac{M_{tot}}{P_0} < 1 + \frac{a}{k}$ (Assumption (23), lower white zone in Figure 9, diagonally hatched zone in Figure 8).

*$c_i(t) \geq 0$ for $t \geq 0$ and all $1 \leq i$ satisfying*

$$v(t) + w(t) + \sum_{i=1}^{\infty} i c_i(t) = v_0 + w_0 + \sum_{i=1}^{\infty} i c_i^0, \qquad \sum_{i=1}^{\infty} c_i(t) = \sum_{i=1}^{\infty} c_i^0, \qquad \forall t \geq 0.$$

*Moreover, by assuming $\sum_{i=1}^{\infty} i^2 c_i^0 < \infty$, then the solution is unique and satisfies*

$$\sup_{t \in [0,T)} \sum_{i=1}^{\infty} i^2 c_i(t) < \infty. \tag{38}$$

The proof of Theorem 2 adapts well-known results of the Becker-Döring system as presented in [3] and is postponed to Appendix C. The main novelty lies in the nonlinearity of the depolymerisation terms, which requires the supplementary assumption for the $b_i$.

### 5.2 Steady states and their local stability

In the following, we assume that the coefficients satisfy

$$\exists\, K > 0 : \qquad \max_{i\geq 1}\left\{\frac{a_i}{i}, \frac{b_i}{i}, \frac{a_i}{b_{i+1}}\right\} \leq K, \qquad \text{and} \qquad a_i > 0, b_{i+1} > 0, \quad \forall i \geq 1. \tag{39}$$

The following result can be seen as the limit as $n \to \infty$ of Proposition 1.

**Proposition 3** (Steady states of the infinite system and their local stability)**.**
*Let $v_0 > 0$, $w_0 > 0$, $P_0 > 0$ and $M_{tot} \geq v_0 + w_0 + P_0 > 0$. Let $(a_i, b_{i+1})_{i\geq 1}$ satisfy* (39).
*Then, there exist the following steady states $(\bar v, \bar w, \bar c_{i\geq 1})$ of the system* (6) *with $n = \infty$:*

*(BSSa) The trivial BSSs $\bar v = \bar w = 0$ and $\bar c_{i\geq 1} \in \ell^1_1$ satisfying*

$$\sum_{i=1}^{\infty} \bar c_i = P_0, \qquad \text{and} \qquad \sum_{i=1}^{\infty} i\bar c_i = M_{tot},$$

*and are always unstable.*

*(BSSb) The BSS $\bar v = M_{tot} - P_0$, $\bar w = 0$, $\bar c_1 = P_0$ and $\bar c_{i\geq 2} = 0$. This steady state is locally asymptotically stable* iff

$$\frac{M_{tot}}{P_0} \leq \frac{a_1}{k} + 1. \tag{40}$$

*(PSS) Under assumption* (40)*, there exists no positive steady state (PSS). Reciprocally, if*

$$\frac{M_{tot}}{P_0} > \frac{a_1}{k} + 1, \tag{41}$$

*there exists a unique PSS $(\bar v, \bar w, \bar c_{i\geq 1})$. Note that as already for the n-polymer model, the stability of the PSS is an open problem.*

**Proof.**
**First step: Existence of the steady states.** After dropping the notation $\bar{\cdot}$ for simplicity, any steady state satisfy

$$kvw = v\sum_{i=2}^{\infty} b_i c_i, \qquad w\sum_{i=1}^{\infty} a_i c_i = kvw, \qquad J_i = J_{i-1} \implies v b_{i+1} c_{i+1} = w a_i c_i, \qquad \forall\, i \geq 1.$$

Let us first suppose $v = 0$. Then, the equation for $w$ implies either $w = 0$ or $c_i = 0$ for all $i$. The first case yields (BSSa) by taking into account the conservation of mass and of the number of polymers. The second case is not possible under the assumption $P_0 > 0$. Hence, (BSSa) gathers all BSSs with $v = 0$.

Next, suppose $v \neq 0$ and $w = 0$. By the equalities $vb_{i+1}c_{i+1} = 0$, we deduce $c_{i\geq 2} = 0$. Consequentially, $c_1 = \sum_{i=1}^{\infty} c_i = P_0$ and $v = M_{tot} - w - \sum_{i=1}^{\infty} ic_i = M_{tot} - P_0$, which is (BSSb).

Let us finally assume both $v \neq 0$, $w \neq 0$. We can divide the equations for $c_i$ by $v$. By denoting $z = \frac{w}{v}$, $\alpha_i = \frac{a_i}{b_{i+1}}$ for $i \geq 1$, $\alpha_0 = 1$, we calculate

$$c_{i+1} = \frac{w}{v}\frac{a_i}{b_{i+1}}c_{i-1} = z\alpha_i c_i = \cdots = z^i c_1 \prod_{j=0}^{i} \alpha_j.$$

Under assumption (39), this series with coefficients $\prod_{j=1}^{i} \alpha_j$ has a strictly positive convergence radius $R$ and since we are looking for steady states in $\ell_1^1$, we consider here only $z < R$. Moreover, the equations for $v$ and $w$ as well as the mass and polymer conservation laws yield the relations:

$$kv = c_1 \sum_{i=1}^{\infty} a_i z^{i-1} \prod_{j=0}^{i-1} \alpha_j, \qquad P_0 = c_1 \sum_{i=1}^{\infty} z^{i-1} \prod_{j=0}^{i-1} \alpha_j,$$

$$M_{tot} = v(1+z) + c_1 \sum_{i=1}^{\infty} iz^{i-1} \prod_{j=0}^{i-1} \alpha_j = c_1 \left( \sum_{i=1}^{\infty} \frac{a_i}{k} z^{i-1}(1+z) \prod_{j=0}^{i-1} \alpha_j + \sum_{i=1}^{\infty} iz^{i-1} \prod_{j=0}^{i-1} \alpha_j \right)$$

We deduce

$$\frac{M_{tot}}{c_1} = \frac{M_{tot}}{P_0} \sum_{i=1}^{\infty} z^{i-1} \prod_{j=0}^{i-1} \alpha_j = \sum_{i=1}^{\infty} z^{i-1} \left( \left( \frac{a_i}{k} + i \right) \prod_{j=0}^{i-1} \alpha_j + \mathbb{1}_{i\geq 2} \frac{a_{i-1}}{k} \prod_{j=0}^{i-2} \alpha_j \right).$$

We recognise a relation of the form $\frac{M}{P_0} F_1(z) = F_2(z)$ and notice that $F_1$ and $F_2$ are two increasing functions in $z$, which are both defined by series with convergence radii $R > 0$. Moreover $F_2$ increases faster than $F_1$ since all its coefficients are strictly larger. Hence, there exists no solution iff $\frac{M_{tot}}{P_0} F_1(0) < F_2(0)$, which is exactly assumption (40). Conversely, if $\frac{M_{tot}}{P_0} F_1(0) \geq F_2(0)$, there exists a unique solution $z < R$, which ensures *a posteriori* the validity of our assumption to only consider $z < R$. Given the solution $z$, the explicit expressions for $c_1$, $v$ and $w$ follow. Note that $z = 0$ in the limit case where $\frac{M_{tot}}{P_0} F_1(0) = F_2(0)$ and we are back to (BSSb).

**Second step: Linear stability or instability of the steady states.** Linearisation of system (6) around the steady states yields the following cases:

1. Linearisation around a state $(0, 0, \bar{c}_i)$: The equation for $v$ gives $\frac{d\widetilde{v}}{dt} = \widetilde{v} \sum_{i=2}^{\infty} b_i \bar{c}_i$, which has the positive eigenvector $(1, 0, c_i = 0)$ for the positive eigenvalue $\lambda = \sum_{i=2}^{\infty} b_i \bar{c}_i$. Hence, these steady states are linearly instable.

2. Linearisation around the state $(M_{tot} - P_0, 0, P_0, c_{i\geq 2} = 0)$. As for the asymptotic stability result, we may pass to the limit $n \to \infty$ in the corresponding proof of Proposition (1).

■

### 5.3 Link with oscillatory models

We proved in the previous section the well-posedness of the infinite model and that there exists a unique positive steady state under assumption (41), which can be interpreted in the way that the initial average size of polymers is "sufficiently large". Proposition 3 leaves the question open if the unique positive steady state is asymptotically stable under this assumption, but we expect this to be true.

In this subsection, in order to give some insights into the question of damped oscillations towards the positive equilibrium, we focus on two specific cases for the parameters of the model: the constant coefficient case and the linear coefficient case. Results for general reaction rate coefficients are difficult and open questions, beyond the scope of this article.

#### The constant coefficient case and its link to a predator-pray Lotka-Volterra system

As for the finite system, assuming constant coefficients permits to derive an explicit formula for the positive steady state.

**Corollary 4** (Non-trivial steady state for constant reaction coefficients)**.**
*Under the assumptions of Proposition 3 with $a_i = a$, $b_i = b$ and under assumption* (41)*, the strictly positive steady state $(\bar{v}, \bar{w}, \bar{c}_{i\geq 1})$ of* (6) *is explicitly given by*

$$\bar{v} = \frac{a}{k}P_0, \qquad \bar{w} = \gamma\frac{b}{k}P_0, \qquad \bar{c}_1 = (1-\gamma)P_0, \qquad \bar{c}_i = \gamma^{i-1}(1-\gamma)P_0, \quad \forall i \geq 2,$$

*where*

$$\gamma = \frac{1}{2}\left(-\frac{a}{b} + \frac{kM_{tot}}{bP_0} + 1 - \sqrt{\left(\frac{a}{b} - \frac{kM_{tot}}{bP_0} + 1\right)^2 + \frac{4k}{b}}\right).$$

**Proof.** The straightforward computations proving Corollary 4 are postponed to Appendix C. ■

*Discussion and biological interpretation:* Corollary 4 supposes assumption (41), which constitutes the biologically most relevant case since from a modelling point of view we are interested in $\frac{M_{tot}}{P_0} \gg 1$, which means that the average size of polymers is initially large, and/or that there are enough monomeric species $v$ and $w$. Accordingly, Corollary 4 states the existence of a PSS, which is conjectured to be stable. The opposite condition (40) concerns cases where the disease cannot spread due to a too small amount of large polymers and monomeric species compared to small polymers (see the discussion for $n$ finite after Proposition 1).

In the case of constant polymerisation coefficients, we obtain the following system

$$\frac{dv}{dt} = -kvw + bv(P_0 - c_1), \qquad \frac{dw}{dt} = -awP_0 + kvw, \qquad \frac{dc_i}{dt} = J_{i-1} - J_i, \qquad 1 \leq i. \quad (42)$$

and observe that if $c_1$ is negligible compared to $P_0$, *i.e.* $P_0 - c_1 \simeq P_0$ with $P_0$ being a constant, then the equations for $(v, w)$ in (42) constitute a Lotka-Volterra system with $v$ taking the role

of the prey and $w$ being the predator. Hence, system (42) can be interpreted as a *perturbed Lotka-Volterra system* in terms of the concentration of the polymer of minimal size $c_1$. Note that this observation is in accordance which the numerically observed oscillations, which are progressively damped towards the steady state and are more pronounced for smaller $c_1$ - the oscillatory behaviour of the system (42) is also reflected in oscillations of $M_1$ and $M_2$ defined by (36).

**The linear coefficient case and its link to a cyclic reaction system**

As in the constant coefficients case, an explicit formula for the positive steady state is easily computed in the case linear polymerisation coefficients.

**Corollary 5** (Non-trivial steady state for linear reaction coefficients)**.**
*Under the assumptions of Proposition 3 with $a_i = ia$, and $b_{i+1} = ib$ for $i \geq 1$, and under assumption* (41)*, the strictly positive steady state $(\bar{v}, \bar{w}, \bar{c}_{i\geq 1})$ of* (6) *is given by*

$$\bar{v} = \frac{a}{k(1-\gamma)}P_0, \qquad \bar{w} = \frac{b\gamma}{k(1-\gamma)}P_0, \qquad \bar{c}_1 = (1-\gamma)P_0, \qquad \bar{c}_i = \gamma^{i-1}(1-\gamma)P_0, \quad \forall i \geq 2$$

*and*

$$\gamma = \frac{M_{tot}k - P_0(a+k)}{M_{tot}k + P_0 b} \in (0,1).$$

**Proof.** Again, we postpone the straightforward calculations of the proof of the corollary to Appendix C. ■

*Discussion and biological interpretation:* Keeping the same notation of the total polymer mass $M_1(t) = M_{tot} - v - w$ as in the previous section, assuming linear polymerisation coefficients yields the simplified system:

$$\frac{dv}{dt} = -kvw + vb(M_1 - P_0), \qquad \frac{dw}{dt} = -waM_1 + kvw, \qquad \frac{dM_1}{dt} = waM_1 - vb(M_1 - P_0). \quad (43)$$

System (43) differs from (42) by featuring an interplay between the two monomer species and the total polymer mass $M_1(t)$, which varies in time as a kind of quasi-variable (and in contrast to total number of polymers $P_0$ being constant).

In situations when $P_0 \ll M_1$ (*i.e.* when the average polymer size remains sufficiently large), we recover the already cited Ivanova differential system (3) in case that $P_0$ is neglected compared to $M_1$. The Ivanova system displays sustained oscillations [28]. In our specific case, the total number of polymers $P_0$ is a perturbation which has an impact on the behaviour of the solutions

of (43). The mass conservation of system (43) implies $M_1(t) = M_{tot} - v(t) - w(t)$. Hence, we can further reduce (43):

$$\begin{cases} \frac{dv}{dt} = -kvw + vb\left((M_{tot} - P_0) - v - w\right), \\ \frac{dw}{dt} = -wa(M_{tot} - v - w) + kvw. \end{cases} \tag{44}$$

The system (44) is a well known quadratic Lotka-Volterra system, see [7] or [15]. By using Poincaré-Bendixson theorem and the Poincaré-Dulac theorem, it follows that solutions of (44) converge to a steady state. Also, the oscillatory behaviour near the steady states follows from the (well-known) eigenvalues of the linearised system. We expect that global oscillatory behaviour of the solutions can be shown by similar arguments as in the two-polymer case, see Corollary 1. Moreover, exponential convergence to the steady state can probably be proven by developing an analog proof as for Theorem 1. These results, however, are beyond the scope of this paper.

## Summary and Perspectives

In this article, we propose a bi-monomeric, nonlinear Becker-Döring-type system, where one monomer species is involved in the polymerisation process while the other monomeric species is able to induce depolymerisation (with an accordingly nonlinear depolymerisation rate). Moreover, the polymerising/depolymerising hierarchy of polymers provides a nonlinear feedback to the evolution of the monomeric species.

A key observation of this paper highlights that the nonlinear coupling between monomeric species and polymer hierarchy leads to generic oscillatory behaviours of solutions, which is in special parametric cases linked to Lotka-Volterra models. A key concept of this paper is that the proposed mathematical model may play a pivotal role in explaining oscillatory behaviour in prion assemblies depolymerisation experiments, and thus become a building block for more specific models for the development of prion diseases.

Furthermore, we performed a full study of the model in the case of only two polymers. We have proven exponential convergence to equilibrium as well as provided an explanation for the damped oscillations, which occur when the monomer dynamics is fast compared to polymerisation/depolymerisation. For the finite and infinite models, we have analysed the existence, uniqueness and stability of the boundary steady states (BSSs) and characterised the existence of positive steady states (PSSs).

Several questions remain open, especially interesting ones for the infinite system: What is the stability of the positive steady state? What is the (nonlinear) rate of convergence to equilibrium? Does a Lyapunov functional exist (at least in a suitable neighbourhood of the PSSs)? How to rigorously prove the existence of damped oscillations?

Turning back to the experiments as shown in Figure 1, it also appears that much remains to be done before reaching a fully quantitative model: integrating the proposed reaction scheme

in a more complete model, where "usual" reactions (like linear depolymerisation) would be the dominant reactions, governing the slow dynamics of the reactions, and these ones local corrections; experimental evidence and quantitative comparison, for instance through data assimilation strategies in the spirit of [1, 2].

Finally, in a similar fashion as the Lifshitz-Slyozov system for Becker-Döring, a continuous approximation of our system could provide interesting insights into the interplay between the different scales, in particular the role of the average size of the polymers, and lead us to new mathematical problems.

**Acknowledgments.** M.D., M.M. and H.R. have been supported by the ERC Starting Grant SKIPPER$^{AD}$ (number 306321). The authors thank Josef Hofbauer for illuminating discussions. K.F. was partially supported by NAWI Graz.

## References

[1] Aurora Armiento, Marie Doumic, Philippe Moireau, and Human Rezaei. Estimation from Moments Measurements for Amyloid Depolymerisation. *Journal of Theoretical Biology*, 397:68–88, March 2016.

[2] Aurora Armiento, Philippe Moireau, Davy Martin, Nad'a Lepejova, Marie Doumic, and Human Rezaei. The mechanism of monomer transfer between two structurally distinct PrP oligomers. *PLoS ONE*, 12(7), July 2017.

[3] John M Ball, Jack Carr, and Oliver Penrose. The Becker-Döring cluster equations: basic properties and asymptotic behaviour of solutions. *Communications in mathematical physics*, 104(4):657–692, 1986.

[4] R. Becker and W. Döring. Kinetische Behandlung der Keimbildung in übersättigten Dämpfen. *Annalen der Physik*, 416(8):719–752, 1935.

[5] M.F. Bishop and F.A. Ferrone. Kinetics of nucleation-controlled polymerization. A perturbation treatment for use with a secondary pathway. *Biophysical Journal*, 46(5):631–644, 1984.

[6] David C Bolton, Michael P McKinley, and Stanley B Prusiner. Identification of a protein that purifies with the scrapie prion. *Science*, 218(4579):1309–1311, 1982.

[7] Immanuel M. Bomze. Lotka-Volterra equation and replicator dynamics: A two-dimensional classification. *Biological Cybernetics*, 48(3):201–211, Oct 1983.

[8] Leonid Breydo, Natallia Makarava, and Ilia V Baskakov. Methods for conversion of prion protein into amyloid fibrils. In *Prion Protein Protocols*, pages 105–115. Springer, 2008.

[9] John Collinge. Prion diseases of humans and animals: their causes and molecular basis. *Annual review of neuroscience*, 24(1):519–550, 2001.

[10] John Collinge and Anthony R. Clarke. A General Model of Prion Strains and Their Pathogenicity. *Science*, 318(5852):930–936, 2007.

[11] Laurent Desvillettes, Kl, and Bao Quoc Tang. Trend to equilibrium for reaction-diffusion systems arising from complex balanced chemical reaction networks. *SIAM Journal on Math. Analysis*, 49(4):2666–2709, 2017.

[12] Klemens Fellner and Bao Quoc Tang. Explicit exponential convergence to equilibrium for nonlinear reaction-diffusion systems with detailed balance condition. *Nonlinear Analysis*, 159:145–180, 2017.

[13] Klemens Fellner and Bao Quoc Tang. Convergence to equilibrium of renormalised solutions to nonlinear chemical reaction-diffusion systems. *ZAMP*, 69:54, 2018.

[14] Pentti Haukkanen and Timo Tossavainen. A generalization of Descartes' rule of signs and fundamental theorem of algebra. *Applied Mathematics and Computation*, 218(4):1203–1207, 2011.

[15] Josef Hofbauer and Karl Sigmund. *Evolutionary games and population dynamics*. Cambridge university press, 1998.

[16] Angélique Igel-Egalon, Mohammed Moudjou, Davy Martin, Alexandra Busley, Tina Knäpple, Laetitia Herzog, Fabienne Reine, Charles-Adrien Richard, Vincent Béringue, Human Rezaei, et al. Reversible unfolding of infectious prion assemblies reveals the existence of an oligomeric elementary brick. *PLoS pathogens*, 13(9):e1006557, 2017.

[17] Mathias Jucker and Lary C Walker. Self-propagation of pathogenic protein aggregates in neurodegenerative diseases. *Nature*, 501(7465):45, 2013.

[18] Jiali Li, Shawn Browning, Sukhvir P Mahal, Anja M Oelschlegel, and Charles Weissmann. Darwinian evolution of prions in cell culture. *Science*, 327(5967):869–872, 2010.

[19] J. Masel, V. A. Jansen, and M. A. Nowak. Quantifying the kinetic parameters of prion replication. *Biophys. Chem.*, 77(2-3):139–152, Mar 1999.

[20] Mathieu Mezache, Marie Doumic, Vincent Béringue, and Human Rezaei. Structural polydispersity of Prion assemblies governs their constitutional dynamic. work in progress.

[21] Oliver Penrose. Metastable states for the becker-döring cluster equations. *Communications in Mathematical Physics*, 124(4):515–541, Dec 1989.

[22] Oliver Penrose and Joel L Lebowitz. Towards a rigorous molecular theory of metastability. *Fluctuation Phenomena*, 7:293–340, 1987.

[23] S. Prigent, A. Ballesta, F. Charles, N. Lenuzza, P. Gabriel, L.M. Tine, H. Rezaei, and M. Doumic. An efficient kinetic model for assemblies of amyloid fibrils and its application to polyglutamine aggregation. *PLoS ONE*, 7(11):e43273, 11 2012.

[24] Joseph B Rayman and Eric R Kandel. Functional prions in the brain. *Cold Spring Harbor perspectives in biology*, 9(1):a023671, 2017.

[25] Gerald Teschl. *Ordinary Differential Equations and Dynamical Systems*, volume 140 of *Graduate Studies in Mathematics*. American Mathematical Society, 2012.

[26] Peter M Tessier and Susan Lindquist. Unraveling infectious structures, strain variants and species barriers for the yeast prion [PSI+]. *Nature Structural and Molecular Biology*, 16(6):598, 2009.

[27] Alasdair Turner. A simple model of the Belousov-Zhabotinsky reaction from first principles. *Bartlett School of Graduate Studies, UCL*, 2009.

[28] Aizik Isaakovich Volpert and Sergei Ivanovich Khudiaev. Analysis in classes of discontinuous functions and the equations of mathematical physics. *Moscow Izdatel Nauka*, 1975.

[29] W-F Xue, S W Homans, and S E Radford. Systematic analysis of nucleation-dependent polymerization reveals new insights into the mechanism of amyloid self-assembly. *PNAS*, 105:8926–8931, 2008.

# A The two-polymer model continued

**Lemma 3** (Local convexity estimate of the Hamiltonian decay)**.**
*Consider as above* $\triangle_\lambda^-$ *to be the interior of the triangle between* $v = 0$ *and the lines* $W_\lambda$ : $w - w_\infty = -\lambda(v - v_\infty)$ *and* $W_\Lambda$ : $w - w_\infty = -\Lambda(v - v_\infty)$.

*Then, for all* $\lambda_\varepsilon < \lambda < 1$ *sufficiently close to one, we have*

$$d^2 - [(v - v_\infty)v_\infty w + (w - w_\infty)vw_\infty]\, p \geq \kappa(v - v_\infty)^2, \tag{45}$$

*for a positive constant* $\kappa = \kappa(\lambda, v_\infty, w_\infty) > 0$.

**Proof.** We set

$$q := [(v - v_\infty)v_\infty w + (w - w_\infty)vw_\infty]$$

and observe that $q > 0$ is equivalent to

$$w - w_\infty \geq -(v - v_\infty)\frac{v_\infty}{v}\frac{w}{w_\infty},$$

where on $\triangle_\lambda^-$ both $\frac{v_\infty}{v} > 1$ and $\frac{w}{w_\infty} > 1$. Hence, the line $q = 0$ is a parabola through the equilibrium $(v_\infty, w_\infty)$ and above the line $p = 0$ which intersects the line $W_\Lambda$ (and thus leaves $\triangle_\lambda^-$) at the point

$$v = \frac{v_\infty(w_\infty + \Lambda v_\infty)}{\Lambda(v_\infty + w_\infty)} < v_\infty.$$

In order to prove (45), we need to estimate $d^2 - qp$ below. Note that $qp > 0$ holds on two subdomains of $\triangle_\lambda^-$: I) the inside of the parabola $q > 0$ up to the line $W_\Lambda$, which we shall denote as $\triangle_{\lambda,I}^-$ and where both $q > 0$ and $p > 0$ and II) the triangle $\triangle_{\lambda,II}^-$ between the lines $W_\lambda$ and $p = 0$, where both $q < 0$ and $p < 0$.

On $\triangle_{\lambda,I}^-$, we estimate $0 \le q \le v_\infty w_\infty p$ with $0 \le p \le (1-\Lambda)(v - v_\infty)$. Together with (14), this implies

$$\text{on } \triangle_{\lambda,I}^- \ : \quad d^2 - qp \ge (v - v_\infty)^2 \left[(w_\infty + \lambda v_\infty)^2 - (1-\Lambda)^2 v_\infty w_\infty\right]$$

By observing that $(1-\Lambda)^2 = (\lambda - 1)^2$, we obtain

$$\kappa = (w_\infty + \lambda v_\infty)^2 - (\lambda - 1)^2 v_\infty w_\infty > 0$$

for $\lambda$ close enough to one.

On $\triangle_{\lambda,II}^-$, where $q < 0$, we estimate

$$\begin{aligned} |q| &= -(v - v_\infty)v_\infty(w - w_\infty) - (w - w_\infty)(v - v_\infty)w_\infty - v_\infty w_\infty p \\ &\le (v - v_\infty)^2(v_\infty + w_\infty)\Lambda - v_\infty w_\infty p. \end{aligned}$$

Since $(1-\lambda)(v - v_\infty) \le p \le 0$ and $(1-\Lambda)^2 = (\lambda - 1)^2$, we obtain

$$\begin{aligned} d^2 - qp &\ge (v - v_\infty)^2 \left[(w_\infty + \lambda v_\infty)^2 + (v_\infty + w_\infty)\Lambda(1-\lambda)(v - v_\infty) - v_\infty w_\infty(\lambda - 1)^2\right] \\ &\ge \kappa(v - v_\infty)^2 \end{aligned}$$

for $\lambda$ close enough to one. ■

**Lemma 4** (Crossing time estimates)**.**
*Consider $\triangle_\lambda^-$ as above. Let $t_1$ be the time when a solution trajectory enters $\triangle_\lambda^-$ at a point $(v_1, W_\Lambda(v_1)$ and $t_2$ the time when the same trajectory leaves $\triangle_\lambda^-$ at a point $(v_2, W_\lambda(v_2))$ with $v_2 < v_1$ and $W_\lambda(v_2) < W_\Lambda(v_1)$.*

*Then, for $\varepsilon$ sufficiently small and all $v_1 \in (0, v_\infty)$, we have that the crossing time is bounded below and above, i.e.*

$$\frac{c_1}{c_2}\frac{1}{2\Lambda[v_\infty + w_\infty]} \le t_2 - t_1 \le \frac{2(\Lambda - \lambda)}{w_\infty}, \tag{46}$$

*where $c_1, c_2 > 0$ are trigonometric constants. Note that $c_1 = O(\lambda - 1)$ while $c_2 = O(1)$.*

**Proof.** We estimate the second equation of (P2) by using that $p \geq (1-\lambda)(v - v_\infty)$, $w_\infty \leq w \leq w_\infty + \Lambda v_\infty$ and $v - v_\infty = -|v - v_\infty|$ holds on $\triangle_\lambda^-$:

$$\begin{aligned} -\dot{w} &= -w(v - v_\infty) + \varepsilon w p \geq w_\infty |v - v_\infty| - \varepsilon(1-\lambda) w |v - v_\infty| \\ &\geq |v - v_\infty| \left[ w_\infty - \varepsilon(1-\lambda)(w_\infty + \Lambda v_\infty) \right] \\ &\geq \frac{w_\infty}{2} |v - v_\infty| \geq \frac{w_\infty}{2} |v_1 - v_\infty|, \end{aligned}$$

where the second last inequality holds for sufficiently small $\varepsilon$, e.g. $\varepsilon \leq \frac{w_\infty}{2(1-\lambda)(\Lambda v_\infty + w_\infty)}$. Hence,

$$w(t_1) - w(t_2) = \int_{t_1}^{t_2} -\dot{w}\, dt \geq \frac{w_\infty}{2} |v_1 - v_\infty| (t_2 - t_1).$$

On the other hand, since $w(t_1) - w(t_2) \leq W_\Lambda(v_1) - W_\lambda(v_1)$ since $v_2 = v(t_2) < v_1 = v(t_1)$, we have

$$w(t_1) - w(t_2) \leq w_\infty - \Lambda(v_1 - v_\infty) - w_\infty + \lambda(v_1 - v_\infty) = (\Lambda - \lambda)|v_1 - v_\infty|$$

which yields the upper bound (46). For the lower bound, we estimate with $w \leq w_\infty + \Lambda v_\infty$

$$\begin{aligned} -\dot{w} &= -w(v - v_\infty) + \varepsilon w p \leq |v - v_\infty| \left[ w_\infty + \Lambda v_\infty \right] (1 + \varepsilon(\Lambda - 1)) \\ &\leq 2\Lambda [v_\infty + w_\infty] |v - v_\infty| \leq 2\Lambda [v_\infty + w_\infty] |v_2 - v_\infty|, \end{aligned}$$

for $\varepsilon$ sufficiently small, e.g. $\varepsilon(\Lambda - 1) \leq 1$. Hence

$$w(t_1) - w(t_2) = \int_{t_1}^{t_2} -\dot{w}\, dt \leq 2\Lambda [v_\infty + w_\infty] |v_2 - v_\infty| (t_2 - t_1) \tag{47}$$

and we require a lower bound for $w(t_1) - w(t_2)$, which we derive as follows. From

$$\begin{aligned} -\dot{v} &= v[w - w_\infty] + \varepsilon v p \leq v_\infty \Lambda |v - v_\infty| + \varepsilon v_\infty (\Lambda - 1) |v - v_\infty| \\ &\leq |v - v_\infty| \Lambda v_\infty \end{aligned}$$

for $\varepsilon$ sufficiently small, e.g. $\varepsilon(\Lambda - 1) \leq \Lambda$ and by recalling $-\dot{w} \geq \frac{w_\infty}{2} |v - v_\infty|$ from above, we estimate

$$\frac{dw}{dv} = \frac{-\dot{w}}{-\dot{v}} \geq \frac{w_\infty}{2\Lambda v_\infty}.$$

The lower bound on $\frac{dw}{dv}$ implies that the solution trajectory starting at $(v_1, w_1 = W_\Lambda(v_1))$ and leaving $\triangle_\lambda^-$ at $(v_2, w_2 = W_\lambda(v_2))$ lies below the straight line $\mathcal{W}$ through $(v_1, w_1)$ with slope $\frac{w_\infty}{2\Lambda v_\infty}$. By denoting $\hat{v}_1, \hat{w}_1$ the crossing between $\mathcal{W}$ and $W_\lambda$, we have that $\hat{v}_1 < v_2 < v_1$ and $\hat{w}_1 > w_2$. Moreover, the length $l$ of $\mathcal{W}$ within $\triangle_\lambda^-$ is proportional both to $v_1 - v_\infty$ and $\hat{v}_1 - v_\infty$ by trigonometric constants. Since $\hat{v}_1 < v_2 < v_1$, $l$ is therefore also proportional to $v_2 - v_\infty$, i.e.

there exist a trigonometric constant $c_1$ such that $l = c_1|v_2 - v_\infty|$. Finally, $l$ is also proportional to $w_1 - \hat{w}_1$, i.e. $l = c_2(w_1 - \hat{w}_1)$. Altogether, that implies that

$$w(t_1) - w(t_2) = w_1 - w_2 \geq w_1 - \hat{w}_1 = \frac{l}{c_2} = |v_2 - v_\infty|\frac{c_1}{c_2},$$

which yields together with (47) the lower bound (46). This finishes the proof. ■

# B Stability of the steady states for the finite system

## Proof of stability of the boundary steady states (Proposition 1)

(BSSa) $v = w = 0$.

To analyse linear stability, we linearise system (6) around those equilibria and obtain the following matrix

$$A_{(0,0)} = \begin{pmatrix} \sum_{i=2}^{n} b_i c_i & 0 & 0 & \cdots & 0 \\ 0 & -\sum_{i=1}^{n-1} a_i c_i & 0 & \cdots & 0 \\ b_2 c_2 & -a_1 c_1 & 0 & \cdots & 0 \\ \cdots & \cdots & 0 & \cdots & 0 \\ b_{i+1}c_{i+1} - b_i c_i & -a_i c_i + a_{i-1}c_{i-1} & 0 & \cdots & 0 \\ -b_n c_n & w a_{n-1} & 0 & \cdots & 0 \end{pmatrix},$$

which has an $n$-fold zero eigenvalue as well as $\lambda_+ = \sum_{i=2}^{n} b_i c_i > 0$ and $\lambda_- = -\sum_{i=1}^{n-1} a_i c_i \leq 0$. Hence, these steady states are always unstable.

(BSSb) $w = c_{i\geq 2} = 0$.

The linearised system is then described by $A_{(v,0)}$ defined by

$$A_{(v,0)} := \begin{pmatrix} 0 & -kv & 0 & b_2 v & \cdots & b_i v & b_{i+1}v & \cdots & b_n v \\ 0 & kv - a_1 P_0 & 0 & 0 & \cdots & 0 & 0 & \cdots & 0 \\ 0 & -a_1 P_0 & 0 & b_2 v & \cdots & 0 & 0 & \cdots & 0 \\ 0 & a_1 P_0 & 0 & -b_2 v & b_3 v & 0 & 0 & \cdots & 0 \\ 0 & 0 & 0 & 0 & \cdots & -b_i v & b_{i+1}v & 0 & 0 \\ 0 & 0 & \cdots & 0 & 0 & 0 & 0 & \cdots & 0 \\ 0 & 0 & \cdots & 0 & 0 & 0 & 0 & 0 & -b_n v \end{pmatrix}.$$

This is exactly symmetric to the case of $A_{(0,w)}$: Zero is an eigenvalue of order two, and the other eigenvalues are $\lambda_i = -b_i v$ for $2 \leq i \leq n$ and $\lambda_1 = kv - a_1 P_0 = kM_{tot} - P_0(k + a_1)$, so that it is unstable iff $M_{tot} > P_0(1 + \frac{a_1}{k})$.

(BSSc) $v = c_{i \leq n-1} = 0$. The linearised system is given by $\frac{dX}{dt} = AX$ with $w = M_{tot} - nP_0$:

$$A_{(0,w)} = \begin{pmatrix} -kw + b_n P_0 & 0 & 0 & \cdots & \cdots & \cdots & 0 & 0 \\ kw & 0 & -a_1 w & \cdots & -a_i w & \cdots & -a_{n-1} w & 0 \\ 0 & 0 & -a_1 w & 0 & 0 & \cdots & 0 & 0 \\ \cdots & \cdots & \cdots & \cdots & \cdots & \cdots & \cdots & \cdots \\ 0 & 0 & \cdots & a_{i-1} w & -a_i w & 0 & \cdots & 0 \\ \cdots & \cdots & \cdots & \cdots & \cdots & \cdots & 0 & 0 \\ b_n P_0 & 0 & 0 & \cdots & 0 & a_{n-2} w & -a_{n-1} w & 0 \\ -b_n P_0 & 0 & 0 & \cdots & 0 & 0 & a_{n-1} w & 0 \end{pmatrix},$$

The eigenvalues are thus 0 (twofold), $\lambda_0 = -kw + b_n P_0$ and $\lambda_i = -a_i w \leq 0$ for $1 \leq i \leq n-1$. This steady state is thus unstable iff $\lambda_0 > 0$, *i.e.* $b_n P_0 > k(M_{tot} - nP_0)$. Note that such a steady state is physically relevant only if it is nonnegative, *i.e.* $M_{tot} \geq nP_0$.

# C The infinite system.

## C.1 Well-posedness

**Proof.**[Theorem 2] **First step: Existence.** Let $x_0^n = (v_0, w_0, c_1^0, \ldots, c_n^0)$. By Lemma 2, system (6) has a unique solution $x^n$ on $[0, \infty)$ with $v^n(t) \geq 0$, $w^n(t) \geq 0$,$c_i^n(t) \geq 0$, for $1 \leq i \leq n$ and

$$v^n(t) + w^n(t) + \sum_{i=1}^{n} i c_i^n(t) = v_0 + w_0 + \sum_{i=1}^{n} i c_i^0, \qquad \sum_{i=1}^{n} c_i(t) = \sum_{i=1}^{n} c_i^0.$$

We construct a sequence $(x^n)_{n \geq 1}$ in $\mathcal{X}$ such that $x^1 = v$, $x^2 = w$, $x^i = c_{i-2}^n, 1 \leq i - 2 \leq n$ and $x^i = 0, \forall i \geq n + 2$. Thus, $\|x^n\|_{\mathcal{X}} \leq \|x_0\|_{\mathcal{X}}$ and $0 \leq v^n(t) \leq \|x_0\|_{\mathcal{X}}$, $0 \leq w^n(t) \leq \|x_0\|_{\mathcal{X}}$, $0 \leq c_i^n(t) \leq i^{-1}\|x_0\|_{\mathcal{X}}, \forall\ t \geq 0$ and all $i$ and $n$. Therefore, using the assumptions on $a_i$, $b_i$, we obtain the bounds

$$|\dot{c}_1^n| \leq \left(a_1 + \frac{b_2}{2}\right) \|x_0\|_{\mathcal{X}}^2,$$

$$|\dot{c}_i^n| \leq \left(\frac{a_{i-1}}{i-1} + \frac{a_i}{i} + \frac{b_{i+1}}{i+1} + \frac{b_i}{i}\right) \|x_0\|_{\mathcal{X}}^2 \leq K_2 < \infty, \qquad i \geq 2.$$

Therefore, for all $i$ the function $c_i^n(.)$ are equicontinuous on $[0, \infty)$. Thanks to the Arzela-Ascoli theorem, we can extract a subsequence $n_k \to \infty$ such that there exists a continuous function

$c_i : [0,\infty) \mapsto \mathbb{R}$ such that $c_i^{n_k} \to c_i$ uniformly on compact subsets of $[0,\infty)$ as $k \to \infty$. Note that $c_i \geq 0$ and $\sum_{i=1}^N i c_i(t) = \lim_{k\to\infty} \sum_{i=1}^N i c_i^{n_k}(t) \leq \|x_0\|_{\mathcal{X}}$. Hence, we obtain

$$\sum_{i=1}^{\infty} i c_i(t) \leq \|x_0\|_{\mathcal{X}}, \qquad \forall t \geq 0. \tag{48}$$

Using the assumptions on $a_i$, $b_i$ and (48), we get

$$\sum_{i=1}^{\infty} a_i c_i(t) \leq K_1 \|x_0\|_{\mathcal{X}} < \infty, \qquad \sum_{i=2}^{\infty} b_i c_i(t) \leq K_2 \|x_0\|_{\mathcal{X}} < \infty, \qquad \forall t \geq 0. \tag{49}$$

Therefore, we also obtain

$$|\dot{v}^n(t)| \leq (k + K_3)\|x_0\|_{\mathcal{X}} \qquad \text{and} \qquad |\dot{w}^n(t)| \leq (k + K_4)\|x_0\|_{\mathcal{X}}.$$

Using the same reasoning and thanks to the the Arzela-Ascoli theorem, there exist continuous functions $v : [0,\infty) \mapsto \mathbb{R}$ and $w : [0,\infty) \mapsto \mathbb{R}$), respectively, such that $v^{n_k} \to v$, (resp. $w^{n_k} \to w$) uniformly on compact subsets of $[0,\infty)$ as $k \to \infty$ and $v \geq 0$, $w \geq 0$.

Finally we pass to the limit as $k \to \infty$ in

$$\begin{aligned}
v^{n_k}(t) &= v_0 + \int_0^t \left( -k v^{n_k}(s) w^{n_k}(s) + v^{n_k}(s) \sum_{i=2}^{\infty} b_i c_i^{n_k}(s) \right) ds, \\
w^{n_k}(t) &= w_0 + \int_0^t \left( -w^{n_k}(s) \sum_{i=1}^{\infty} a_i c_i^{n_k}(s) + k v^{n_k}(s) w^{n_k}(s) \right) ds, \\
c_1^{n_k}(t) &= c_i^0 + \int_0^t \left( - a_1 c_1^{n_k}(s) w^{n_k}(s) + b_2 c_2^{n_k}(s) v^{n_k}(s) \right) ds, \\
c_i^{n_k}(t) &= c_i^0 + \int_0^t \left( (a_{i-1} c_{i-1}^{n_k}(s) - a_i c_i^{n_k}(s)) w^{n_k}(s) + (b_{i+1} c_{i+1}^{n_k}(s) - b_i c_i^{n_k}(s)) v^{n_k}(s) \right) ds, \quad i \geq 2.
\end{aligned}$$

We get (37) at the limit thanks to the uniform convergence and the bounds obtained in (49).

Moreover, in order to obtain a priori estimates (38), we compute:

$$\frac{d}{dt} \sum_{i=1}^{n_k} i^2 c_i^{n_k} = \sum_{i=1}^{n_k - 1} (2i+1)(a_i w^{n_k} c_i^{n_k} - b_{i+1} v^{n_k} c_{i+1}^{n_k}).$$

Using the bounds on $w^{n_k}$, $v^{n_k}$ and the assumptions on $a_i$, $b_{i+1}$, we get

$$\sum_{i=1}^{n_k} i^2 c_i^{n_k} \leq \sum_{i=1}^{\infty} i^2 c_i^0 + K \left( \int_0^t \sum_{i=1}^{n_k} i^2 c_i^{n_k} \right),$$

where the constant $K$ is independent of $k$. Since $\sum_{i=1}^{\infty} i^2 c_i^0 < \infty$ and using Gronwall's inequality we get:

$$\sum_{i=1}^{l} i^2 c_i^{n_k} + \sum_{i=l+1}^{n_k} i^2 c_i^{n_k} \leq M e^{Kt},$$

for all $t \geq 0$ where $M$ is a constant independent of $k$. Letting $k \to \infty$ then $l \to \infty$, we deduce

$$\sum_{i=1}^{\infty} i^2 c_i \leq M e^{Kt}$$

and (38).

We can also obtain the following conserved quantities for the solution of the system (6) with $n = \infty$. Since (37) holds, we get for $n > 1$, $t \geq 0$

$$\sum_{i=1}^{n} c_i(t) - \sum_{i=1}^{n} c_i^0 = -\int_0^t J_n(s) ds.$$

Since $v$, $w$ are bounded and (49), we have $\lim_{n\to\infty} -\int_0^t J_n(s) ds = 0$ and

$$\sum_{i=1}^{\infty} c_i(t) = \sum_{i=1}^{\infty} c_i^0.$$

We also have

$$\sum_{i=1}^{n} i c_i(t) - \sum_{i=1}^{n} i c_i^0 = \int_0^t \sum_{i=1}^{n} i \left(J_{i-1}(s) - J_i(s)\right) ds = -\int_0^t n J_n(s) ds + \int_0^t \sum_{i=1}^{n-1} J_i(s) ds, \qquad (50)$$

and

$$\sum_{i=n+1}^{\infty} c_i(t) - \sum_{i=n+1}^{\infty} c_i^0 = \int_0^t J_n(s) ds.$$

We obtain the following result from (48)

$$\lim_{n\to\infty} (n+1) \sum_{i=n+1}^{\infty} c_i(t) \leq \lim_{n\to\infty} \sum_{i=n+1}^{\infty} i c_i(t) = 0,$$

whence $\lim_{n\to\infty} \int_0^t n J_n(s) ds = 0$. Then, by passing to the limits and adding $v$, $w$ to (50) we obtain

$$v(t) + w(t) + \sum_{i=1}^{\infty} i c_i(t) = v_0 + w_0 + \sum_{i=1}^{\infty} i c_i^0. \qquad (51)$$

**Second step: Uniqueness.** Let $x_1 = (v_1, w_1, c)$ and $x_2 = (v_2, w_2, d)$ be absolutely continuous in time solutions of system (6) with $n = \infty$ and the same initial condition $x_0 = (v_0, w_0, c_0)$. Then, we note

$$J_i^{(1)} = a_i w_1 c_i - b_{i+1} v_1 c_{i+1}, \qquad J_i^{(2)} = a_i w_2 d_i - b_{i+1} v_2 d_{i+1}, \quad \forall i \geq 1$$

and $J_0^{(1)} = J_0^{(2)} = 0$. Let $V(t) = v_1(t) - v_2(t)$, $W(t) = w_1(t) - w_2(t)$ and $y_i(t) = c_i(t) - d_i(t)$. Then, for a.e. $t \in [0, T)$ we have

$$\begin{aligned}
\frac{d}{dt}|V| + |W| &= \operatorname{sign}(V)\bigg(-kVw_1 - kv_2W + V\sum_{i=2}^{\infty} b_i c_i + v_2 \sum_{i=2}^{\infty} b_i y_i\bigg) \\
&\quad + \operatorname{sign}(W)\bigg(kv_1W + kVw_2 - W\sum_{i=1}^{\infty} a_i c_i - w_2 \sum_{i=1}^{\infty} a_i y_i\bigg), \\
&= |V|\bigg(-kw_1 + \operatorname{sign}(VW)kw_2 + \sum_{i=2}^{\infty} b_i c_i\bigg) + |W|\bigg(kv_1 - \operatorname{sign}(VW)kv_2 - \sum_{i=1}^{\infty} a_i c_i\bigg) \\
&\quad + \bigg(\operatorname{sign}(V)v_2 \sum_{i=2}^{\infty} b_i y_i - \operatorname{sign}(W)w_2 \sum_{i=1}^{\infty} a_i y_i\bigg).
\end{aligned}$$

We have by (49) and (51) that

$$\frac{d}{dt}|V| + |W| \leq K_1 \left(|V| + |W| + \sum_{i=1}^{\infty} i|y_i|\right). \tag{52}$$

Integrating (52) we obtain for $t \in [0, T)$

$$|V(t)| + |W(t)| \leq K_1 \int_0^t \left(|V| + |W| + \sum_{i=1}^{\infty} i|y_i|\right) ds. \tag{53}$$

We also have for a.e. $t \in [0, T)$

$$\frac{d}{dt}\sum_{i=1}^{n} i|y_i| = \sum_{i=1}^{n} (J_i^{(1)} - J_i^{(2)})[(i+1)\operatorname{sign}(y_{i+1}) - i\operatorname{sign}(y_i)] - (n+1)\operatorname{sign}(y_{n+1})(J_{n+1}^{(1)} - J_{n+1}^{(2)}). \tag{54}$$

Now

$$\begin{aligned}
(J_i^{(1)} - J_i^{(2)})[(i+1)\operatorname{sign}(y_{i+1}) - i\operatorname{sign}(y_i)] &= (a_i y_i w_1 + a_i d_i W - b_{i+1} y_{i+1} v_1 - b_{i+1} d_{i+1} V) \\
&\quad \times [(i+1)\operatorname{sign}(y_{i+1}) - i\operatorname{sign}(y_i)], \\
&= a_i w_1 |y_i|[(i+1)\operatorname{sign}(y_{i+1} y_i) - i] - b_{i+1}|y_{i+1}|v_1[(i+1) - i\operatorname{sign}(y_{i+1} y_i)] \\
&\quad + (a_i d_i W - b_{i+1} d_{i+1} V)[(i+1)\operatorname{sign}(y_{i+1}) - i\operatorname{sign}(y_i)],
\end{aligned}$$

hence

$$(J_i^{(1)} - J_i^{(2)})[(i+1)\,\mathrm{sign}(y_{i+1}) - i\,\mathrm{sign}(y_i)] \le a_i w_1 |y_i| + (2i+1)(a_i d_i |W| + b_{i+1} d_{i+1} |V|). \quad (55)$$

Integrating (54) and using (55), we therefore obtain for $t \in [0,T)$

$$\begin{aligned} \sum_{i=1}^{n} i|y_i| \le \int_0^t \sum_{i=1}^{n} a_i w_1 |y_i| ds + \int_0^t \sum_{i=1}^{n} (2i+1)(a_i d_i |W| + b_{i+1} d_{i+1} |V|) ds \\ - (n+1) \int_0^t \mathrm{sign}(y_{n+1})(J_{n+1}^{(1)} - J_{n+1}^{(2)}) ds. \end{aligned} \quad (56)$$

Using the assumption on $a_i,\ b_{i+1}$ we have by (38) that

$$\sup_{t\in[0,T)} \sum_{i=1}^{\infty} (2i+1) a_i d_i(t) < \infty, \qquad \sup_{t\in[0,T)} \sum_{i=1}^{\infty} (2i+1) b_{i+1} d_{i+1}(t) < \infty. \quad (57)$$

By the same arguments as in the first step, we deduce

$$\lim_{n\to\infty} (n+1) \int_0^t \mathrm{sign}(y_{n+1})(J_{n+1}^{(1)} - J_{n+1}^{(2)}) ds = 0, \quad t \in [0,T). \quad (58)$$

Using (56)–(58), $a_i = O(i)$ and letting $n \to \infty$, we therefore obtain for $t \in [0,T)$

$$\sum_{i=1}^{\infty} i|y_i|(t) \le K_2 \int_0^t \left( |V| + |W| + \sum_{i=1}^{\infty} i|y_i| \right) ds. \quad (59)$$

Summing the two inequalities (53) and (59) and using Gronwall's inequality, we obtain that

$$|V(t)| + |W(t)| + \sum_{i=1}^{\infty} i|y_i(t)| = 0, \qquad t \in [0,T)$$

and thus $(v_1, w_1, c) = (v_2, w_2, d)$ and uniqueness. ■

## C.2 Explicit formula for the positive steady state.

**Proof.**[Corollary 4] We define $\gamma = \frac{a}{b} z = \alpha z$ and use the expressions obtained in the Proposition 3

$$\bar{c}_i = \gamma^{i-1} \bar{c}_1, \qquad \tfrac{\bar{c}_1}{1-\gamma} = P_0, \qquad k\bar{v} = a \tfrac{\bar{c}_1}{1-\gamma} = aP_0,$$

$$\bar{v} + \bar{w} + \tfrac{\bar{c}_1}{(1-\gamma)^2} = \tfrac{a}{k} P_0 + \tfrac{b\bar{v}\gamma}{a} + \tfrac{P_0}{1-\gamma} = P_0 \left( \tfrac{a}{k} + \tfrac{b\gamma}{k} + \tfrac{1}{1-\gamma} \right) = M_{tot},$$

which gives us immediately a second-order equation for $\gamma$: We define

$$\beta_1 = \frac{b}{k}, \quad \beta_2 = \frac{a}{k}, \qquad \mu = \frac{M_{tot}}{P_0}.$$

We have

$$\tfrac{a}{k}(1-\gamma) + \tfrac{b}{k}\gamma(1-\gamma) + 1 = \tfrac{M_{tot}}{P_0}(1-\gamma),$$

$$\beta_2(1-\gamma) + \beta_1\gamma(1-\gamma) + 1 = \mu(1-\gamma),$$

$$\beta_1\gamma^2 + \gamma(\beta_2 - \mu - \beta_1) + \mu - 1 - \beta_2 = 0,$$

We calculate the discriminant

$$\Delta = (\beta_2 - \mu - \beta_1)^2 - 4\beta_1(\mu - 1 - \beta_2) = (\beta_2 - \mu + \beta_1)^2 + 4\beta_1,$$

$$\gamma_\pm = \tfrac{1}{2}\left(-\tfrac{\beta_2}{\beta_1} + \tfrac{\mu}{\beta_1} + 1 \pm \sqrt{(\tfrac{\beta_2}{\beta_1} - \tfrac{\mu}{\beta_1} + 1)^2 + \tfrac{4}{\beta_1}}\right).$$

We see easily that for any value of the parameters we have $\gamma_+ > 1$: Indeed, we have

$$\gamma_+ > \frac{1}{2}\left(-\frac{\beta_2}{\beta_1} + \frac{\mu}{\beta_1} + 1 + |\frac{\beta_2}{\beta_1} - \frac{\mu}{\beta_1} + 1|\right) \geq 1.$$

Thus, the only admissible solution is $\gamma_-$. We see similarly that it is always smaller than 1

$$\gamma_- < \frac{1}{2}\left(-\frac{\beta_2}{\beta_1} + \frac{\mu}{\beta_1} + 1 - |\frac{\beta_2}{\beta_1} - \frac{\mu}{\beta_1} + 1|\right) \leq 1.$$

And we have $\gamma_- > 0$ under the assumption (41). ■

**Proof.**[Corollary 5] Using the same notations as previously, we have

$$\gamma = \frac{a\bar{w}}{b\bar{v}}, \qquad \bar{c}_i = \gamma^{i-1}\bar{c}_1, \qquad \frac{\bar{c}_1}{1-\gamma} = P_0,$$

and denoting $f(\gamma) = \frac{1}{1-\gamma} = \sum_{i=0}^{\infty} \gamma^i$

$$k\bar{v} = a\bar{c}_1 \sum_{i=1}^{\infty} i\gamma^{i-1} = aP_0(1-\gamma)f'(\gamma) = \frac{aP_0}{(1-\gamma)}, \qquad k\bar{w} = bc_1 \sum_{i=1}^{\infty} i\gamma^i = \frac{bP_0\gamma}{(1-\gamma)}$$

$$\bar{v} + \bar{w} + \frac{c_1}{(1-\gamma)^2} = \frac{aP_0}{k(1-\gamma)} + \frac{bP_0\gamma}{k(1-\gamma)} + \frac{P_0}{(1-\gamma)} = M_{tot},$$

and thus

$$M_{tot}k(1-\gamma) = P_0(a + b\gamma + k), \qquad \gamma = \frac{M_{tot}k - P_0(a+k)}{M_{tot}k + P_0 b} < 1.$$

We have $\gamma > 0$ iff the assumption (41) is fulfilled. ■

# D Materials and methods of the depolymerisation experiment shown in Figure 1

Formation of amyloid fibrils: PrP amyloid fibrils were formed using the manual setup protocol described previously in [8]. Fibril formation was monitored using a ThT binding assay [8]. Samples were dialysed in 10 mM sodium acetate, pH 5.0. Then fibrils were collected by ultracentrifugation and resuspended in 10 mM sodium acetate, pH 5.0. A washing step was performed by repeating the ultracentrifugation and resuspension steps in 10 mM sodium acetate, pH 5.0. Static light scattering: Static light scattering kinetic experiments were performed with a thermostatic homemade device using a 407-nm laser beam. Light-scattered signals were recorded at a $112^0$ angle. Signals were processed with a homemade MatLab program. All experiments have been performed at $55^0$C in a 2mmX10mm cuve.